Energy Reports 14 (2025) 2700–2719

Contents lists available at ScienceDirect

Energy Reports

journal homepage: www.elsevier.com/locate/egyr

Research paper

Bi-level framework for cost effective robustness and responsiveness to enhance infrastructure resilience of transmission network against cyclones

Abhishek Kumar Gupta [a], Kusum Verma [a], Sachin Sharma [b,*]

[a] Department of Electrical Engineering, Malaviya National Institute of Technology, Jaipur, Rajasthan 302017, India
[b] Department of Electrical and Electronics Engineering, Manipal Institute of Technology, Manipal Academy of Higher Education, Manipal, Karnataka 576104, India

ARTICLE INFO

Keywords:
Cyclones
Fragility
High impact low probability (HILP) events
Infrastructure resilience
Resilience metrics
Responsiveness
Robustness

ABSTRACT

Power system transmission infrastructures are becoming vulnerable to the adverse effects of High Impact Low Probability (HILP) events such as the extreme weather conditions leading to their structural damage and prolonged outages. This requires more attention for making a robust and resilient power grid. This paper proposes a bi-level framework for quantitative assessment of resilience of transmission lines using different resilience metrics based on the multi-state resilience curve when the system subjected to severe cyclonic events of different intensities. The system is divided into high, medium, and low wind speed regions observed during a given cyclone. These regions are mapped over the fragility curves of the transmission lines to obtain their failure probabilities using Monte Carlo Simulation (MCS). The robustness and responsiveness of transmission line infrastructure is estimated to determine enhanced ability of the transmission line to withstand and recover from such events. Different economic metrics and costs are proposed for estimated robustness and responsiveness. Sensitivity analysis is performed for economic viability of proposed hardening parameters to enhance the infrastructural resilience. The proposed methodology is investigated on transmission networks resilience studies on IEEE 57 bus system to understand the impact of such catastrophic events during planning stage. Results show that resilience metrics such as Load Not Served (LNS) and Energy Not Served (ENS) have decreased with proposed robustness levels for improved structural hardening. The economic benefits have resulted in reduction of total failure cost by over 35 % with 10 % increase in robustness and nearly 68 % with 20 % robustness respectively.

1. Introduction

Electricity is one of the most critical infrastructures affecting nation's economic growth and well-being. The existence and development of adequate infrastructure are essential for the country's economy's sustained growth. Therefore, critical infrastructure, such as the electricity sector, is a prime candidate for developing adaptive, resilient strategies to address vulnerabilities brought about by climate change (Yodo and Arfin, 2021; Liu et al., 2024). Globally, extreme weather occurrences have increased significantly during the past ten years (Gupta and Verma, 2024). According to data NCEI, between 2017 and 2023, the United States experienced 137 distinct billion-dollar disasters, resulting in over 5500 fatalities and causing more than $1 trillion in damages. A major factor in these costs is the landfall of Category 4 or 5 hurricanes in the U. S. in five of the past seven years (Bolan et al., 2024). In U.S. at least 50, 000 customers have been affected over the past two decades due to the extreme weather events. The frequency of cyclones over the Arabian Sea has increased by 52 % during the past two decades, according to the Indian Institute of Tropical Meteorology (Baburaj et al., 2022), approximate 1.1 billion USD damaged cost has been estimated in power transmission and distribution system due to cyclone in Odisha (Mohanty et al., 2020). These data of climate change impact noticeably indicate that the power sector needs more robust infrastructure to provide an uninterrupted power supply. Many severe hazards, such as natural hazards like floods, ice storms, extreme windstorms, wildfires and Earthquakes attacks has challenged the resilience of the modern power grids (Tian et al., 2023). The growing frequency and intensity of extreme weather events, such as cyclones, has exposed the inherent vulnerabilities of transmission networks, leading to large-scale outages, cascading failures, and significant socio-economic losses (Wang et al., 2022a).

* Correspondence to: Department of Electrical and Electronics Engineering, Manipal Institute of Technology, Manipal Academy of Higher Education, Manipal, Karnataka, India.
E-mail address: sachin.sharma@manipal.edu (S. Sharma).

https://doi.org/10.1016/j.egyr.2025.09.014
Received 30 June 2025; Received in revised form 25 August 2025; Accepted 20 September 2025
Available online 27 September 2025

Resilience is defined "the ability of the system to absorb shocks and reduce the magnitude or duration of disruptive events. It can also anticipate, absorb, adapt to, and/or rapidly recover from such an event (Stanković et al., 2023). Transmission systems, as critical lifelines linking generation and demand, face unique risks from high-speed winds, flooding, and storm surges that can damage towers, lines, and substations, thereby threatening overall system stability (Wang et al., 2022a). Recent resilience studies emphasize that improving infrastructure resilience requires a multiphase approach encompassing proactive preparedness, rapid responsiveness, and adaptive recovery (Mujjuni et al., 2023). There is a strong need to focus more on the power system infrastructural and operational research during catastrophic events to ensure the robustness and resiliency of the system.

Fig. 1 conceptually highlights the critical role of a reliable and resilient power grid in supporting essential societal functions such as healthcare, transportation, communication, businesses, and households. It shows that resilience is not only a technical characteristic but also a socio-economic necessity, underpinning quality of life, economic productivity, and the integration of renewable and digital technologies. In the context of cyclones, where large-scale transmission network disruptions can jeopardize these essential services, the figure emphasizes the urgent need for strategies that enhance both robustness (through preventive design and infrastructural hardening) and responsiveness (through rapid recovery and adaptive operations). This paper proposed a bi-level framework aligns with this perspective by providing a cost-effective means to strengthen physical infrastructure while ensuring swift operational responses, thereby safeguarding critical services and societal wellbeing during and after extreme weather events. In this study, resilience is treated as a time-dependent property capturing both robustness: the ability to resist wind-induced failures, modeled via design wind thresholds and fragility and responsiveness: the speed and effectiveness of post-event repair and restoration. Together, these levers determine the area under the resilience curve, expected energy not served (ENS), and the economic consequences of outages.

1.1. Literature survey and critical review

The field of resilience assessment has seen significant advancements in recent years, focusing on quantifying the ability of critical infrastructure systems to withstand disruptions and recover effectively (Zhuang and Xie, 2024; Zeng et al., 2024). Several metrics-based methods have been proposed for assessment of the resilience (Lee et al., 2024; Amrovani et al., 2025). It may be based on their performance or attributes (Bhusal et al., 2020; Umunnakwe et al., 2021). Ref (Gama Dessavre et al., 2016), presented a multidimensional framework for resilience that integrates system performance throughout time, establishing a basis for conceptualizing resilience as a dynamic process. In (Sharma et al., 2018), mathematical formulations were established to represent recovery processes, highlighting the necessity for stochastic resilience metrics that can adjust to diverse recovery curves. These contributions have established a foundation for resilience modeling but frequently lack an integrated emphasis on robustness (resistance to failure) and responsiveness (recovery speed), both essential for assessing infrastructure performance during catastrophic events such as cyclones.

The role of component fragility models in resilience assessment has been highlighted in studies Dunn et al. (2018) and Guidotti et al. (2016), who explored network interdependencies and cascading effects following disruptions. These works underscore the importance of robustness and have not covered comprehensive evaluations of recovery dynamics. Authors in ref (Ouyang and Dueñas-Osorio, 2014), further advanced the field by integrating fragility models with restoration strategies in hurricane-prone regions, focusing on probabilistic resilience assessment for power systems. However, while these studies provide valuable insights into failure probabilities and network vulnerabilities, they mainly address isolated aspects of resilience and often lack a unified framework to evaluate robustness and responsiveness across all phases of disruption and recovery.

Another area of focus in the literature is the validation of resilience methodologies using real-world systems. While in (Ouyang and Dueñas-Osorio, 2014), applied resilience metrics to the Harris County power grid, and other studies utilized simplified networks or single-event scenarios, there remains a gap in applying these methods to complex, real-world benchmarks like the IEEE 57 or any standard IEEE test system. Additionally, the variability in repair times and its impact on recovery metrics are often overlooked, limiting the applicability of these methods in understanding system responsiveness under diverse hazard scenarios (Sharma et al., 2018).

However, despite methodological advances in modeling fragility, repair dynamics, and disaster scenarios, these works often lack a detailed integration of economic analysis, particularly in evaluating the cost-effectiveness of robustness and responsiveness strategies. They do not quantify resilience investments using metrics such as Benefit-to-Cost Ratio (BCR), Cost-Effectiveness Ratio (CER), or Resilience Efficiency Index (REI), nor do they explore how sensitivity to economic parameters like value of lost load (VOLL) or hardening cost affects decision-making.

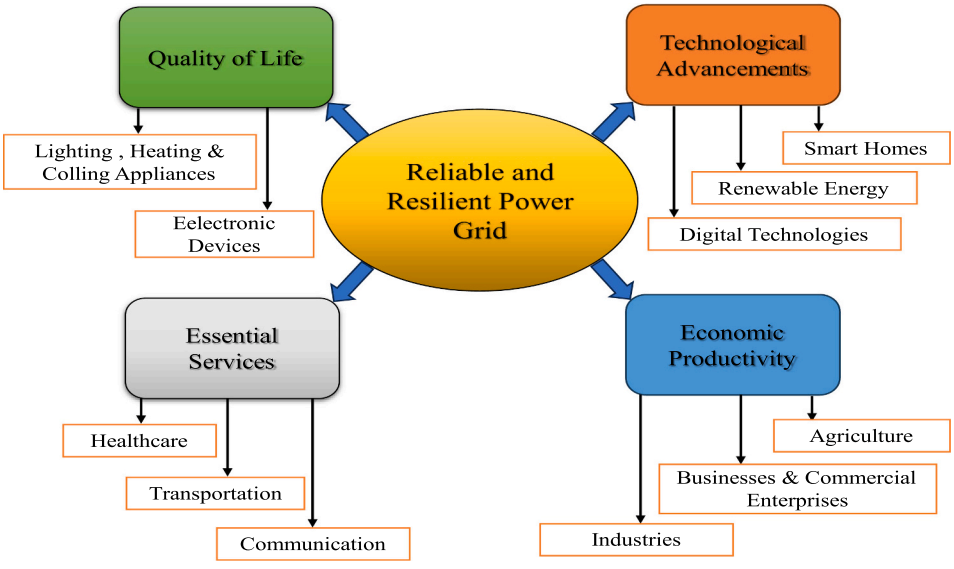

Fig. 1. Critical Role of Reliable and Resilient Power Grid.

While prior resilience studies focus on outage mitigation, few evaluate the economic trade-offs involved in infrastructure hardening. This work addresses this gap by quantifying the cost-benefit and sensitivity analysis of resilience strategies, thus guiding informed investments. This highlights a critical gap in resilience research, necessitating a cohesive framework that bridges these limitations and provides actionable insights for real-world infrastructure resilience.

This paper addresses following gaps: lack of a unified, bi-level framework that jointly quantifies robustness and responsiveness across cyclone phases: limited cost-integrated models that combine hardening cost, response cost, and failure cost; limited sensitivity analysis of key economic drivers and limited benchmark validation under realistic cyclone zoning. In this paper, a bi-level multi-state resilience framework is developed for transmission lines exposed to cyclonic hazards. At Level-1, robustness is quantified by adjusting the design wind speed within fragility modeling, thereby capturing the capacity of transmission lines to resist wind-induced damage. At Level-2, responsiveness is evaluated by modifying the repair time, representing the efficiency of post-event restoration. A comprehensive cost formulation is introduced. To assess the economic efficiency of resilience strategies, multiple performance indicators are used, including outage cost savings, Resilience Efficiency Index, Cost-Effectiveness Ratio, and the Benefit-to-Cost Ratio. Furthermore, a sensitivity analysis is performed by varying the unit hardening cost, the Value of Lost Load, the increment in design wind speed and the number of lines hardened. The proposed framework is demonstrated on the IEEE-57 bus transmission system, with high, medium and low-wind regions.

Table 1 presents the comparison between existing research in literature and the proposed work. While existing studies in ref (Gama Dessavre et al., 2016). and (Sharma et al., 2018) emphasize the importance of time-dependent metrics for describing system performance during and after disruptions, they fall short in providing a structured framework that comprehensively evaluates robustness and responsiveness. Ref (Guidotti et al., 2016). and (Ouyang and Dueñas-Osorio, 2014) incorporated component fragility models to assess failure probabilities and resistance without integrating a unified resilience framework applicable across all phases of a hazard. Although some methodologies employ probabilistic tools like Monte Carlo Simulation for failure analysis, their application to real-world power systems under specific hazards, such as cyclones, remains limited (Gama Dessavre et al., 2016; Sharma et al., 2018). The author of ref (Ouyang and Dueñas-Osorio, 2014). has not discussed robustness and responsiveness, however, proposed a probabilistic resilience framework and some metrics to evaluate the resilience of substation. These studies have focused on resilience assessment and enhancement of power systems under extreme events such as typhoons and multi-type disasters. In ref (Wang et al., 2022b). authors proposed a planning-oriented resilience assessment framework for integrated electricity-gas systems using impact-increment state enumeration, while in (Yang and Li, 2022) authors introduced a hybrid data-model-driven approach to assess transmission line vulnerability using multi-factor modeling. Moreover, (Resilience-oriented Transmission, 2024) integrated optimal transmission switching into resilience expansion planning for typhoon scenarios. In (Liu and Xie, 2024), authors proposed probabilistic resilience assessment framework specifically for ultra-high-voltage (UHV) converter stations subjected to seismic events. Their methodology integrated four modules: a matrix-based conditional probability model to quantify functional states between nodes, an improved Bayesian network to capture connectivity and power transmission reliability, a stepped functional recovery function to simulate the time-varying recovery trajectory after an earthquake, and an economic loss model that quantified monetary impacts of disruptions.

Table 1
Comparison of proposed methodology with existing research on aspects of resilience studies.

Ref.	Events	System Application	Resilience Metrics	Robustness	Responsiveness	Cost-Benefit Analysis	Sensitivity Analysis	Resilience Enhancement Strategies
(Gama Dessavre et al., 2016)	General disruptions	Simulated complex networks	Multi-dimensional resilience metrics based on stress-strain relationships	×	×	×	×	Visualization tools for dominance and design optimization
(Sharma et al., 2018)	Earthquake	Engineering systems (e.g., bridges)	Area under recovery curves, incorporating stochastic shocks	✓	✓	×	×	Proposes mathematical resilience metrics
(Guidotti et al., 2016)	Seismic hazards and cascading effects	Potable water and power networks	Functionality metrics based on interdependency modeling	✓	×	×	×	Suggests prioritization of restoration and mitigation strategies
(Ouyang and Dueñas-Osorio, 2014)	Hurricane hazards	Harris County power grid	Resilience as ratio of performance (area under system performance curve)	✓	✓	×	×	Evaluates effectiveness of robustness and rapidity improvements
(Wang et al., 2022b)	Multi-type natural disasters	IEEE RTS 79 EPS	Resilience Index (RI) via impact-increment process	✓	✓	×	×	Redundancy planning, multiple dispatch strategies
(Yang and Li, 2022)	Typhoon disasters	IEEE RTS 79	Data-driven resilience performance scores (hybrid fragility models)	✓	×	×	×	Component hardening, fragility reduction
(Resilience-oriented Transmission, 2024)	Typhoon weather	IEEE 30	Expected Unserved Energy (EUE),	✓	×	✓	×	Transmission switching, line expansion planning
(Liu and Xie, 2024)	Seismic hazards	800 kV-substation	Seismic resilience index	×	×	×	×	Probabilistic
[Proposed]	Cyclones	IEEE 57-bus system	Multi-state metrics capturing robustness, responsiveness, ENS, LNS, RA	✓	✓	✓	✓	Bi-Level with robust-response trade-offs, cost modeling

✓: Considered, ×: Not Considered

1.2. Major contributions

The proposed work directly addresses these limitations by introducing a multi-state resilience framework that quantifies robustness and responsiveness through novel metrics. It employs Monte Carlo Simulation (MCS) to assess failure probabilities using fragility curves mapped to wind speed data, thereby providing a stochastic yet practical approach to resilience assessment under cyclonic conditions. Additionally, the framework is validated on the IEEE 57 bus system, a standard yet complex benchmark for power network studies, demonstrating its applicability to real-world systems. By adjusting fragility curves and repair times by ±10 % and ±20 %, the methodology uniquely evaluates robustness and responsiveness across various scenarios, offering actionable insights for enhancing the resilience of transmission networks. The major contributions of this work are as follows:

- A bi-level multi-state resilience framework is developed to quantifies resilience through distinct resilience metrics across cyclone progression, degradation, and restoration phases.
- The framework uniquely quantifies robustness and responsiveness of transmission lines using fragility curves and repair times under varying windstorm intensities.
- Monte Carlo Simulation is used to determine the failure probabilities of transmission lines under varying wind intensities, providing a probabilistic approach to understanding system vulnerabilities during extreme weather events.
- A novel cost-integrated resilience model is proposed by integrating robustness, responsiveness, and outage costs to assess trade-offs in resilience strategies.
- A detailed sensitivity analysis is performed on key parameters including unit cost to increase design wind speed of line due to hardening (α), value of lost load (VOLL), and increase in design wind speed due to hardening (Δv_{des}), revealing the most influential factors affecting the economic viability of resilience strategies.
- The proposed methodology is applied to the IEEE 57 bus transmission network, demonstrating its practical applicability and validating the framework for real-world power system resilience assessment under catastrophic events.

2. Mathematical modeling

2.1. Modeling of cyclone

The historical wind data utilized for this study was sourced from the Indian Meteorological Department (IMD) (Regional Specialized, 2023), (A Report on Extremely Severe Cyclonic Storm FANI over the Bay of Bengal 26 April to 4 May, 2019). Specific data for Cyclone Fani was obtained from the IMD's official website. Cyclone intensity was measured using a 3-minute sustained wind speed recorded at a standard height of 10 m above ground level. Cyclone Fani exhibited a peak maximum sustained wind (MSW) ranging between 200 and 210 km/h (approximately 55.6–58.3 m/s), with a total duration of up to 7 days (168 h) (Singh et al., 2021).

To support resilience analysis, the cyclonic wind field was divided into three intensity zones: High Wind Region (HWR), Medium Wind Region (MWR), and Low Wind Region (LWR). This classification allows for a systematic evaluation of windstorm impacts on infrastructure systems across spatially distinct zones. The categorization is based on wind speed thresholds, enabling a region-specific understanding of cyclone dynamics. The mathematical representation of cyclonic wind fields involves the following components:

The wind speed 'v_i' for a specific region 'i' is determined using a scaling factor 's_i' relative to the cyclone's maximum sustained wind speed 'v^{max}':

$$v_i = s_i . v^{max} \tag{1}$$

where s_i is the scaling factor, with typical values $s_{HWR} = 1.1$, $s_{MWR} = 0.9$ and $s_{MWR} = 0.7$; v^{max} is the peak maximum sustained wind speed of the cyclone.

The total wind exposure 'E_i' for a region over the duration of the cyclone 'T' is expressed as

$$E_i = \int_0^T v_i(t)dt \tag{2}$$

where $v_i(t)$ is the time dependent wind speed for region 'i'. The wind force F (in Newtons) acting on a structure is derived from the wind pressure P, given by

$$P = \frac{1}{2}\rho v_i^2 \tag{3}$$

where ρ is the air density ($\sim 1.225 kg/m^3$ at sea level). The Force F acting on a structure with a projected area A (in m^2) and dimensionless drag coefficient C_d is given as

$$F = C_d . A . P \tag{4}$$

Transmission Line Fragility Modeling

Regional weather conditions greatly affect the resilience of transmission lines. Depending on its durability and ability to survive the windstorm, it may hold or collapse. Different fragility curves are needed for each transmission line of the system to model transmission line failure. Analytical, experimentation, historical data, expert opinion, and a mix of these methods are used to create fragility curves (Gupta and Verma, 2022). The fragility function is expressed by Eq. (6) (Lian et al., 2023), allowing the mapping of time-series weather profiles to obtain weather-affected failure probabilities at each simulation step. This dynamic approach captures the evolving weather conditions realistically.

$$P_{TL}^{v_i} = \begin{cases} 0 if v_i < v_{Cr} \\ \exp\left[\frac{\lambda(v_i - v_{Cr})}{v_{Cr}}\right] - 1 if v_{Cr} < v_i < v_{Col} \\ 1 if v_i > v_{Col} \end{cases} \tag{5}$$

where v_I is the wind speed in the region i (HWR, MWR, LWR), v_{Cr} is the critical wind speed (30 m/s), below which no failure occurs, v_{Col} is the collapse wind speed (60 m/s), above which failure is certain (Trakas et al., 2016). λ= 0.6391 is taken from ref (Lian et al., 2023).

The failure probability P_f of transmission line in a specific region is determined by mapping the wind speed v_I to its fragility curve:

$$P_f = f(v_i) \tag{6}$$

where $f(v_i)$ represents the cumulative probability of failure at wind speed v_i. This mapping allows for the dynamic assessment of failure probabilities as the cyclone progresses.

2.2. Monte Carlo Simulation (MCS) based transmission line failure analysis

The Monte Carlo Simulation (MCS) is a mathematical technique used to estimate the probable outcomes of uncertain events by leveraging computational simulations. It analyses large datasets to predict outcomes that are influenced by random variables. In the context of MCS, the probability of different outcomes is modeled for processes or systems where precise predictions are difficult due to inherent variability and uncertainty. By employing random sampling, MCS generates numerous potential scenarios, enabling the estimation of average results and the identification of probabilistic trends, providing robust insights into complex systems (Billinton and Li, 1994). Monte Carlo Simulation (MCS) is employed to analyse the probabilistic failure of transmission

lines under time-series wind speed data, scaled for specific regions (HWR, MWR, LWR).

A random number '𝕣' is drawn from uniform distribution (𝕣 ∼ U (0,1)) for each transmission line. The failure status F_{TL} is determined by comparing the failure probability P_f with the random number 𝕣 :

$$F_{TL} = \begin{cases} 0 if P_f < \mathbb{r} \\ 1 if P_f > \mathbb{r} \end{cases} \quad (7)$$

where $P_f > \mathbb{r}$, then the transmission line fails to operate. If $P_f < \mathbb{r}$, then the transmission line will remain in operational state. The system-wide failure probability P_{sys} is calculated by aggregating the probabilities across all regions. Assuming the failure events are independent, the system-wide failure probability is given by:

$$P_{sys} = 1 - \prod_i (1 - P_f(v_i)) \quad (8)$$

The above steps are repeated for a large number of iterations N to account for all possible outcomes. The system-wide failure probability is then averaged over all iterations:

$$\widehat{P}_{sys} = \sum_{k=1}^{N} P_{sys}^{(K)} \quad (9)$$

where $P_{sys}^{(K)}$ is the failure probability in the k-th iteration.

2.3. Time to repair

The time to repair R_{time} shows the time require to repair a fallen line, i.e., the time required by the repair crew to reach the affected area, replace the damaged components to restore the service of the tripped components. A different R_{time} for the transmission lines is required. The R_{time} of these components under low weather R_{base} may increase with higher wind speeds as the overall damage also increases and subsequently accessibility of the affected areas is affected. Based on the transmission line's past failures and the time needed to repair the damaged line, system operators typically provide a repair time. R_{base} is the normal repair time of the transmission line when maximum wind speed is under 20 m/s, and it is considered to be 10 h for the transmission line (Lindsey,). Three damage level are defined in different wind region here as follows:

$$\begin{cases} Low\ damage\ if v_i^{\max} \le 20\frac{m}{s} \\ Moderate\ damage\ if 20\frac{m}{s} < v_i^{\max} \le \frac{45m}{s} \\ High\ damage\ if 20\frac{m}{s} < v_i^{\max} \le 70\frac{m}{s} \end{cases} \quad (10)$$

Thus, time to repair transmission line for these damage levels is determined by Eq. (12)

$$R_{time} = k\left(v_i^{\max}\right).R_{base} \quad (11)$$

where $k\left(v_i^{\max}\right)$ dynamically selects the multiplier based on the wind intensity region. It is defined as:

$$k\left(v_i^{\max}\right) = \begin{cases} 1 if v_i^{\max} \le 20\frac{m}{s} \\ k_a if 20\frac{m}{s} < v_i^{\max} \le \frac{45m}{s} \\ k_b if 20\frac{m}{s} < v_i^{\max} \le 70\frac{m}{s} \end{cases} \quad (12)$$

The repair time increases with wind intensity. For wind speeds between 20 m/s and 45 m/s, it is calculated as $k_a.R_{base}$ where $k_a \sim U(2,4)$. For wind speeds between 45 m/s and 70 m/s, it is given by $k_a.R_{base}$ where $k_b \sim U(5,7)$. These ranges k_a and k_b are adopted from reference (Panteli et al., 2017), and they account for the increased repair effort required as the wind intensity rises.

3. Proposed methodology

3.1. Multi state resilience curve

A simplified version of the conceptual resilience curve developed as a multi-state resilience curve as depicted in Fig. 2 to define and quantify power system resilience. It shows that the resilience level is a time-dependent function for a given extreme event. Time dependent metrics is proposed in this paper for each transition period i.e., for state-II, state-III and state-IV for quantify the infrastructure resilience. As shown in Fig. 2, it is divided into five states (Stanković et al., 2023):

3.1.1. Initial resilient state

State-I is the initial resilient state. It is assumed that the 100 % transmission lines are in 'on' state and resilience level in this state is denoted by RL_i. It may be possible at initial level some of transmission lines are in off state, therefore, resilience level can be marked accordingly.

3.1.2. Event progress state

In state-II, windstorm occurs at time, t_1 because of that resilience level drops from initial resilience level, RL_i. Event starts on time t_1 and end on time t_2. Event progress from t_1 to t_2. The initial infrastructure resilience level RL_i is assumed to be 100 % and equal to number of intact transmission lines lying in the respective wind speed region.

The number of transmission lines tripped per day and the number of transmission lines in service per day is determined using (13) and (14) respectively.

Number of transmission line tripped per day is given as:

$$TL_{trip} = \sum F_{TL} \quad (13)$$

It represents the number of transmission lines tripped per day and F_{TL} denotes the failure status of transmission line which can be obtained by (7).

The number of transmission lines in service per day is given as:

$$TL_{ser} = RL_i - \sum F_{TL} \quad (14)$$

It shows number of transmission line remained in service per day and RL_i is initial infrastructure resilience level.

During state-II, the resilience level drops from initial resilience level, RL_i to post event degraded state resilience level, RL_p. In state-II two resilience metrics proposed as follows

$$TL_{dl} = RL_i - RL_p \quad (15)$$

where, TL_{dl} is transmission line degradation level i.e., how many transmissions line is tripped and RL_p is post event degraded state resilience level, RL_i is initial infrastructure resilience level.

Metrics R_{hour} is calculated by (16) by evaluating the slope of degradation level as shown in Fig. 1 during state-II. It gives a rate at which the resilience level falls from the initial level.

$$R_{hours} = -\frac{TL_{dl}}{t_{hour}} \quad (16)$$

where t_{hour} can be calculated as: $t_{hour} = t_2 - t_1$

Degradation State

State-III is a post event degraded state following the end of the

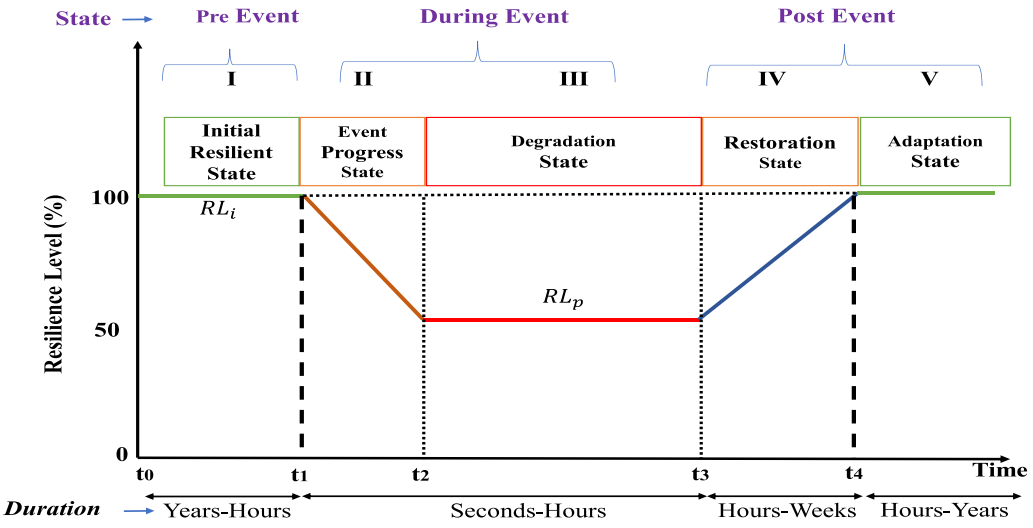

Fig. 2. Multi State Resilience Level Curve.

extreme event and before the restoration process is initiated for infrastructure resilience. Resilience level in this state is RL_p known as post event degraded state resilience level. Level of RL_p depend on the intensity of event. If intensity is low or high, its level may be increased or decreased accordingly. Duration of state-III is t_2 to t_3. It may be less or more depending upon the nature of severity of the event. The duration of degradation state can be evaluated by the metric as

$$R_{dr} = t_3 - t_2 \tag{17}$$

where R_{dr} is resilience metric during degraded state indicating the number of hours or day the transmission lines will remain in off state even after the windstorm has ended.

Restoration State

State -IV is a restorative state. In this state, restoration of transmission lines started at time t_3 and ended at time t_4. The duration of the restorative period depends on the availability of the crew. It may vary from a few hours to a few days, depending on the impact of the catastrophic event on the system. The R_{rs} metric is defined during restorative state, and it is obtained by the slope during state-IV shown in Fig. 2 as

$$R_{rs} = \frac{TL_{dl}}{t_{rh}} \tag{18}$$

where t_{rh} can be calculated as $t_{rh} = t_4 - t_3$

3.1.3. Adaptation state

State-V is adaptation state. It accomplishes after restoration of all the necessary system facility. Final level of resilience may be equal, high or low depending upon the new strength of infrastructures.

3.2. Area-based resilience metrics

Resilience metrics for area under curves are proposed for state-II ($R_{Area_{II}}$), state-III ($R_{Area_{III}}$) and state-IV ($R_{Area_{III}}$) and it is obtain by Eqs. (19), (20) and (21) respectively and overall resilience area metric ($R_{Area}^{Overall}$) is obtained by (22) as

$$R_{Area_I} = \int_{t_1}^{t_2} \left(\frac{(RL_p - RL_i)(t - t_1)}{t_2 - t_1} + RL_i \right) dt \tag{19}$$

$$R_{Area_{II}} = \int_{t_2}^{t_3} (RL_i - RL_p)\, dt \tag{20}$$

$$R_{Area_{III}} = \int_{t_3}^{t_4} \left(\frac{(RL_i - RL_p)(t - t_3)}{t_4 - t_3} + RL_p \right) dt \tag{21}$$

$$R_{Area}^{Overall} = R_{Area_I} + R_{Area_{II}} + R_{Area_{III}} \tag{22}$$

4. Proposed bi-level resilience framework

The proposed methodology aims to assess the resilience of a transmission network during cyclonic events, focusing on two critical attributes: robustness and responsiveness. The methodology integrates these attributes across different resilience states to provide a comprehensive assessment of the system performance. While robustness and responsiveness represent two distinct aspects of system resilience, their effects are interdependent and can complement or compensate for one another. Robustness aims to minimize the occurrence of failures by hardening infrastructure, while responsiveness focuses on minimizing the duration of service interruption after failures occur. In practice, an increase in robustness reduces the number of tripped lines during cyclonic events, thereby lowering the burden on the recovery process. Conversely, if some failures are unavoidable, enhanced responsiveness ensures that the system returns to normal faster, reducing the energy not served (ENS) and the area under the degraded state in the resilience curveThe framework begins with data acquisition, including weather forecasts, infrastructure characteristics, and system operational parameters. The proposed bi-level resilience framework is structured into two interdependent levels. Level 1 focuses on robustness-based system strength and Level 2 focuses on the responsiveness-based recovery speed.

4.1. Level-1: robustness-based system strength (fragility layer)

Level-1 models the system's ability to resist initial failure during extreme wind events by adjusting the fragility characteristics of transmission lines through structural hardening measures (e.g., raising wind speed thresholds). Robustness is estimated by analysing the network's ability to withstand initial disruptions, including the calculation of tripped transmission lines and degraded resilience levels. This layer captures the physical vulnerability and strength of the infrastructure.

Table 2
Robustness Levels.

Case Study	Robustness Level (H_j)
20 % Less Robust	H_1
10 % Less Robust	H_2
Base Case	H_3
10 % More Robust	H_4
20 % More Robust	H_5

Table 3
Response Levels For + 10 % Robust Case Scenarios.

Case Study	Robustness Level (S_j)	Δ_{resp}
20 % Less Response	S_1	+ 0.2
10 % Less Response	S_2	+ 0.1
Base Case	S_3	0
10 % More Response	S_4	− 0.1
20 % More Response	S_5	− 0.2

The following cases are considered:

4.1.1. Base case

Resilience quantification is modelled with the help of multi-state resilience curve for windstorms of different intensities. For the base case, the cyclone-1 has three regions with wind speeds of 65 m/s, 54 m/s, 42 m/s and cyclone-2 are having three regions with wind speeds of 45 m/s, 41 m/s, 33 m/s respectively.

4.1.2. Robust case

Robustness is the ability of a system or infrastructure to resist damage and maintain its functionality when exposed to external stresses or extreme events. It reflects the inherent strength and structural capacity to withstand adverse conditions without significant degradation. It can be achieved through hardening. Hardening directly impacts the fragility curve by increasing critical wind speed thresholds (v_{Cr}), the wind speed at which failure begins and collapse thresholds (v_{Col}), the wind speed at which complete failure occurs. By adjusting these parameters, the robustness level of the infrastructure is enhanced, delaying the onset of fragility and extending the point of catastrophic failure. For instance, hardening measures such as reinforcing transmission towers, using higher-grade materials, or improving structural designs can raise v_{Cr} and v_{Col}, resulting in fragility curves that reflect improved resistance to failure. This approach allows for the evaluation of robustness scenarios, such as 10 % or 20 % increased robustness, where the critical and collapse thresholds are proportionally scaled upwards. Conversely, decreased robustness due to aging or lack of maintenance can similarly be modeled by reducing these thresholds. These adjustments provide a quantitative framework to assess and compare the resilience of transmission networks under varying robustness levels as mentioned in Table 2.

a. With increased robustness (10 % or 20 % more robust):

$$v_{cr}^{H_j} = v_{cr}^{base}.(1+\Delta k) \tag{23}$$

$$v_{col}^{H_j} = v_{col}^{base}.(1+\Delta k) \tag{24}$$

Where H_j represents robustness (hardening) level. Δk is incremental robustness factor (0.1 and 0.2).

b. With decreased robustness (10 % or 20 % less robust):

$$v_{cr}^{H_j} = v_{cr}^{base}.(1-\Delta k) \tag{25}$$

$$v_{col}^{H_j} = v_{col}^{base}.(1-\Delta k) \tag{26}$$

Using the adjusted $v_{cr}^{H_j}$ and $v_{col}^{H_j}$, the fragility curve for each robustness level is obtained by using Eq. (6).

4.2. Level-2: responsiveness-based recovery speed (response layer)

Level-2 in contrast, focuses on how quickly the system can recover after damage has occurred. Responsiveness is evaluated by monitoring recovery efforts, which include the duration of the degraded state and the restoration rate of the transmission lines. It evaluates the impact of improving response mechanisms such as reducing repair times and enhancing restoration capacity. Together, these levels provide a comprehensive view of resilience by combining both preventive (robustness) and corrective (responsiveness) adaptation strategies. The following cases are considered:

4.2.1. Responsive case

Responsiveness measures the ability of a system to recover swiftly from disruptions, such as cyclonic windstorms, and restore its operational state. For transmission networks, responsiveness depends on the time required to repair damaged components, including the accessibility of affected areas and the efficiency of restoration processes. By adjusting the repair time (R_{Time}), different responsiveness scenarios can be modeled, ranging from faster recovery (e.g., 10 % or 20 % quicker repair) to slower recovery (e.g., 10 % or 20 % delayed repair).

This parameter provides insights into the system's adaptability and efficiency in minimizing downtime and restoring resilience. The repair time for each responsiveness level (S_j) is modelled as:

$$R_{base}^{S_j} = R_{base}.(1+\Delta_{resp}) \tag{27}$$

where Δ_{resp} is responsiveness factor representing the percentage change in repair time. R_{base} is a repair time under normal condition. The robust case scenarios having 10 % more robustness levels are considered for further investigating the responsiveness of transmission lines to the impact of the windstorm by defining the different response levels (S_j) for both the robust cases as mentioned in Table 3. A similar study can be conducted for other robustness levels to evaluate the impact of varying responsiveness on resilience metrics across different wind regions.

Fig. 3 illustrates the proposed methodology for assessing the resilience of a transmission network during cyclonic events.

4.3. Resilience assessment algorithm

The resilience assessment algorithm for a transmission network under cyclones systematically evaluates the network's performance during and after the impact of extreme weather events. It begins by identifying the initial infrastructure resilience level (RL_i) and monitoring the failure status of transmission lines (F_{TL}) in real-time to compute the number of lines tripped and in service. Key dynamic metrics, such as the degradation rate, restoration rate, and duration of degraded states, are calculated for each phase. The algorithm also computes resilience areas under each state's curve to quantify the system's overall resilience. By integrating these metrics, the algorithm provides a comprehensive time-dependent resilience profile, enabling informed decision-making for pre-event preparation and post-event recovery of transmission networks.

Algorithm. Resilience Assessment of Transmission Network Against Cyclones

1. *Initialize Parameters:*
   - Set initial time t = 0; Set wind region index i = 1
   - Define simulation duration T
   - Define wind regions: High Wind Region (HWR), Medium Wind Region (MWR), Low Wind Region (LWR)
2. *Calculate Failure Probability Using Fragility Curves:*
   for each transmission line in the network
   - Map wind speed data to fragility curve
   - Calculate failure probability of transmission line using Monte Carlo Simulation (MCS) (Eq. 6)

   end
3. *Determine Transmission Line Status:*
   for each transmission line
   - Generate a random number r between 0 and 1

     If (failure probability > r) *THEN*
     Set transmission line status to "off" (failed state)
     else
     Set transmission line status to "on" (operational state)
     end

   end
4. *Calculate Repair Time for Failed Lines:*
   for each transmission line in "off" state
   - Calculate repair time R_{Time} based on wind speed and region (Eq. 11)

   end
5. *Update IEEE 57 Bus System:*
   - Update the status of each transmission line in the IEEE 57 bus system according to the respective wind region (HWR, MWR, LWR)
6. *Calculate Daily and Hourly Transmission Line Metrics*:
   for each day and each hour in T
   - Calculate TL_{trip} (Eq. 13) for lines that failed within the day/hour.
   - Calculate TL_{ser} (Eq. 14) for lines that remained operational.

   end
7. *Evaluate Resilience Metrics for Multi-State Resilience Curve:*
   for each state (II, III, IV)
   - Calculate resilience metrics for each state:
     - State II-IV (Eq. 13-18)
     - Area Metrics (Eq. 19-22)

   end
8. *Robustness Analysis by Adjusting Fragility Curves: Level-1: Robustness-Based System Strength*
   for each robustness level (±10%, ±20%)
   - Adjust fragility curve for transmission line robustness. (Eq. 23-26)
   - Repeat Steps 2-7 for each robustness scenario.

   end
9. *Responsiveness Analysis by Modifying Repair Time*: *Level-2: Responsiveness-Based Recovery Speed*
   for each responsiveness level (±10%, ±20%)
   - Modify repair time T_{repair} by adjusting it ±10% and ±20%. (Eq. 27)
   - Repeat Steps 2-8 for each responsiveness scenario.

   end
10. *Compute Cost Components:*
    for each Scenario
    - Calculate total cost (Eq. 28-31)
    - Calculate economic evaluation metrics (Eq. 32-38)

    end
11. *Perform Sensitivity Analysis* (Eq. 39)

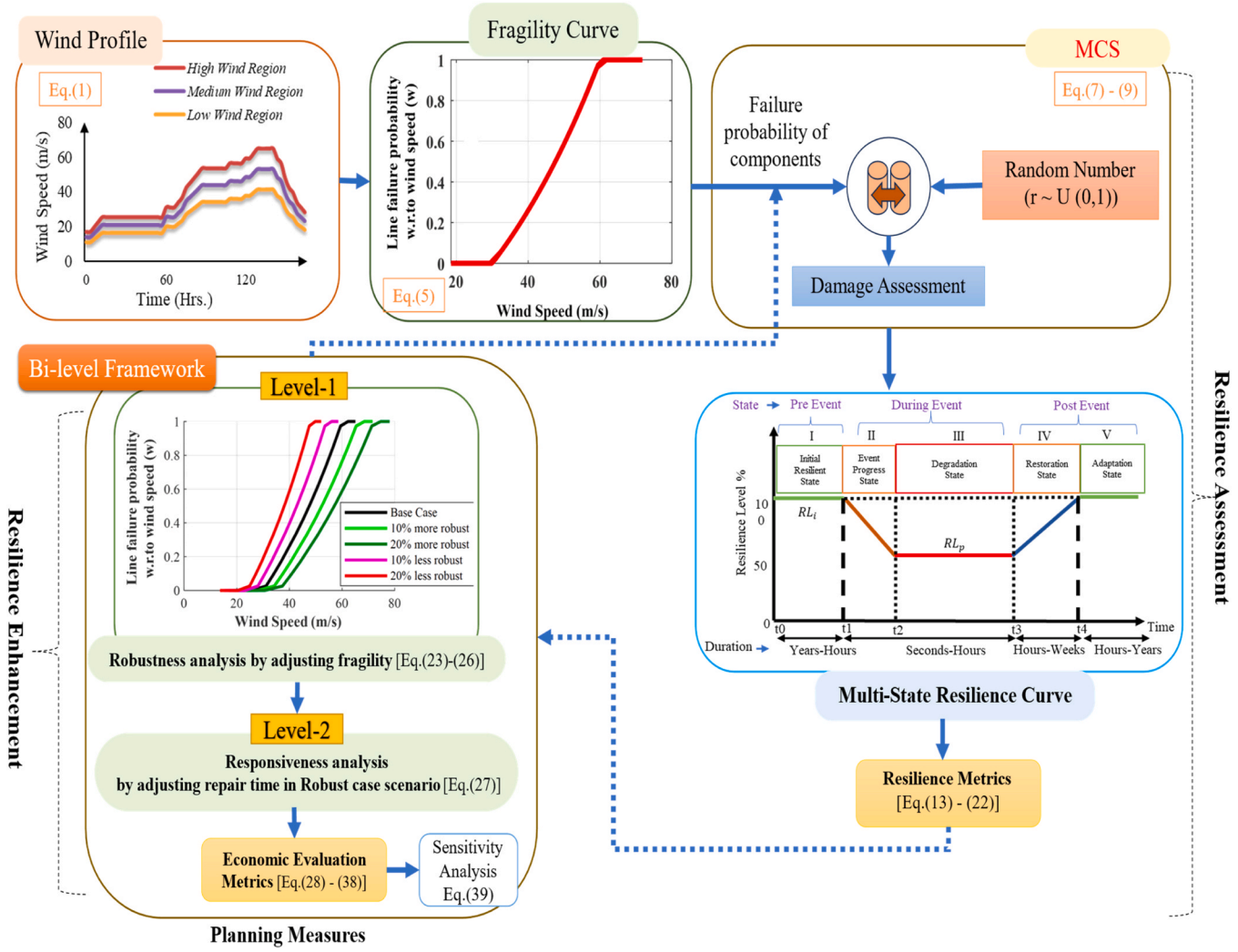

Fig. 3. Proposed bi-level framework to estimate cost effective robustness and responsiveness for enhanced transmission network resilience.

5. Proposed cost modeling and economic evaluation

Enhancing power system resilience through robustness (infrastructure hardening) and responsiveness (faster recovery) requires significant investment. Decision-makers must evaluate the trade-offs between cost and resilience gains to ensure optimal allocation of limited resources. This section introduces a cost-benefit analysis (CBA) model to assess the economic feasibility of resilience strategies under cyclonic events.

5.1. Proposed total cost computation

The total cost C_{Tot} for resilience strategy is calculated by:

$$C_{Tot} = C_{rob} + C_{resp} + C_{fail} (\$/\text{km}) \tag{28}$$

Where C_{rob} is cost of hardening infrastructure, C_{resp} is cost of enhancing responsiveness and C_{fail} is cost of outages due to component failures.

5.1.1. Robustness cost

Robustness cost indicates strength of the transmission line that can withstand the increased wind speed during cyclones after hardening, defined as

$$C_{rob} = \sum_{i=1}^{N} \alpha_i . \Delta v_{des,\ i} (\$/\text{km}) \tag{29}$$

where α_i is cost per unit increase in design wind speed for line i by 1 m/s and $\Delta v_{des,i}$ is increase in design wind speed in m/s due to line hardening. Design wind speed, $v_{des,i}$ refers to the engineered wind speed tolerance of transmission line i, beyond which the line is likely to suffer damage or failure. It reflects the structural capability of the asset to withstand high wind loads as defined by design standards or robustness enhancements. The increase in design wind speed $\Delta v_{des,i}$, represents the extent of hardening applied to line i. This increment directly drives the robustness cost, computed by Eq. (29).

5.1.2. Responsiveness cost

Responsiveness cost indicates reduction in the transmission line repair time after improved robustness, defined as

$$C_{resp} = \sum_{j=1}^{M} \beta_j . \Delta r_j (\$/\text{km}) \tag{30}$$

where β_j (USD/(km-hr.)) is cost per unit reduction in repair time for transmission line j and Δr_j (hr.) is reduction in average repair time.

5.1.3. Failure cost

It is total economic cost experienced due to unserved electrical load when transmission lines fail during the cyclonic events.

$$C_{fail} = \sum_{t=1}^{T} L_t.VOLL.\quad h_t(\$/\text{km}) \tag{31}$$

where L_t is Load Not Served (LNS) (in MW) at time t due to line failures, $VOLL$ is Value of Lost Load ($/MWh) and h_t is Time duration (in hours) of disruption.

5.2. Proposed economic evaluation metrics

5.2.1. Benefit metric

It represents the economic advantage gained by implementing resilience strategies, expressed as the difference between the baseline outage cost and the total cost under the resilience strategy. It is proposed as

$$B_{net} = |C_{fail,base} - (C_{fail} + C_{rob} + C_{resp})(\$/\text{km}) \tag{32}$$

A positive value of B_{net} indicates a favourable resilience investment. Where $C_{fail,base}$ is the total outage cost experienced in the baseline scenario, where no resilience enhancements (such as robustness or responsiveness upgrades) have been implemented in the transmission system and outage cost saving can be evaluated using Eq. (33)

$$\text{Outage Cost Saving} = C_{fail,base} - C_{fail}(\$/\text{km}) \tag{33}$$

Cost-Benefit Trade-Off Curve

To illustrate trade-offs, a cost vs. resilience gain plot can be generated. Resilience gain can be represented by the decrease in total outage duration or increase in area under the resilience curve.

$$\textit{Resilience Gain}, RG = RA_{strategy} - RA_{base} \tag{34}$$

$$RA_{strategy} = ENS_{Base} - ENS_{strategy}(\text{MWh}) \tag{35}$$

The Resilience Area (RA) in each scenario is computed as the difference between the Energy Not Served (ENS) in the baseline case and that in the strategy scenario. This metric reflects the additional energy preserved that is how much more energy is served (or less energy lost) due to robustness improvements.

5.2.2. Cost effective ratio (CER)

The Cost Effectiveness Ratio (CER) provides a metric to assess the efficiency of resilience investments by comparing the total cost incurred to the resilience gain achieved. It is defined as the ratio of the total resilience cost to the resilience gain RG, which represents the reduction in energy not served (ENS) relative to the baseline scenario. A lower CER indicates a more economically efficient strategy, as it implies a greater resilience improvement per unit cost. This metric supports decision-making by highlighting strategies that offer the best trade-off between cost and resilience enhancement.

$$CER = \frac{C_{Tot}}{RG}(\$/\text{km} - \text{MWh}) \tag{36}$$

5.2.3. Benefit-to-cost ratio (BCR)

The Benefit-to-Cost Ratio (BCR) is a key indicator used to evaluate the economic justification of resilience investments. It is defined as the ratio of the outage cost saving to the combined cost of robustness and responsiveness measures, expressed as:

$$BCR = \frac{\text{Outage Cost Saving}}{C_{rob} + C_{resp}} = \frac{C_{fail,base} - C_{fail}}{C_{rob} + C_{resp}}(\text{unitless}) \tag{37}$$

A BCR greater than 1 indicates that the investment yields more in avoided outage costs than it incurs in resilience expenditures, making it economically favourable. This ratio enables comparative assessment of different strategies and helps prioritize interventions that offer the highest return on resilience investment.

Resilience Efficiency Index (REI):

The Resilience Efficiency Index (REI) quantifies the amount of resilience benefit gained per unit of investment. It is defined as the ratio of the resilience gain (measured as MWh of Energy Saved) to the total resilience cost.

$$REI = \frac{RG}{\textit{Total Cost}(\text{MWh}/\$/\text{km})} \tag{38}$$

This metric provides a direct measure of how efficiently resilience upgrades convert financial input into improved system performance. Higher REI values indicate more effective use of resources, helping stakeholders identify strategies that deliver maximum resilience for each dollar spent.

6. Simulation and results

In this study, the proposed bi-level resilience framework is investigated on the standard IEEE 57 bus transmission system to investigate the impact of windstorms of different intensities on the transmission line resilience. It includes both physical resilience outcomes and economic assessments with a focus on understanding how robustness and responsiveness affect system performance and cost-effectiveness.

6.1. Test system

IEEE 57 bus transmission system has 80 transmission lines, 57 buses, 42 load and 7 generators which are connected at bus number 1, 2,3, 6, 8, 9, and 12 having total generation capacity of 1278.7 MW and load demand of 1250.8 MW. IEEE Standard 57 bus system is divided into three regions based on the wind speed intensity and direction from sea to land as shown in Fig. 4. It is also seen from the line diagram that some of the transmission lines overlap in two different wind profile regions. The failure of all such lines is considered according to the worst wind profile region in which they are present. It is assumed that the windstorm is cyclonic in nature and lasts for a period of one week. The impact of cyclonic windstorm hitting the transmission network is taken from the end of 2nd day till the 7th day and the total duration of windstorm for these 5 days is 120hrs. Table 4 shows the number of transmission lines lying in these three-wind speed regions.

6.2. Fragility curves of transmission line

Fig. 5 shows the fragility curve of transmission lines of IEEE 57 bus system considered in this paper. Five robustness level cases as mentioned in Table 4 are evaluated including base case for understanding the resilience in terms of robustness of transmission line to resist the damage and continue operating during the cyclone.

6.3. Impact of different cyclones on resilience of transmission lines

The resilience of overhead transmission lines can be affected by different characteristics of extreme events. Cyclones of varying intensities are considered in this paper as shown in Table 5 to quantitatively evaluate the resilience performance of transmission lines using various metrics proposed in Section 3.

6.4. Resilience of transmission lines during cyclone-1

Cyclone-1 data, sourced from the Indian Meteorological Department (IMD), is detailed in Section 2. Based on the modeling framework described in Section 2, Cyclone-1 is visually represented in Fig. 6.

The number of transmission lines tripped/day (5) considering robustness for cyclone-1 on IEEE 57 bus system is shown in Fig. 7 for period of five days (D1-D5 for 120Hrs). Fig. 7 shows the cumulative number of transmission lines tripped per day for cyclone-1. It is considered here that if a transmission line fails on day1(D1), then it will remain in this failed state for all remaining days until recovery action is

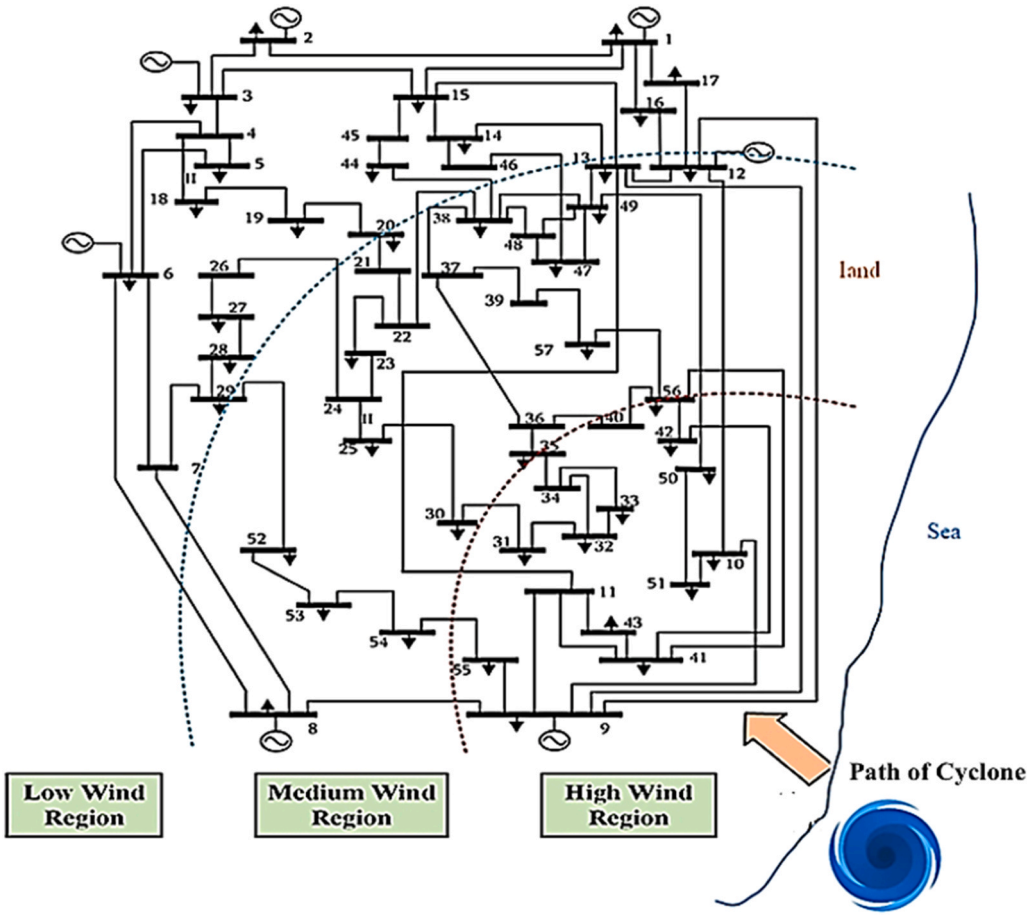

Fig. 4. Line diagram of IEEE 57 Bus Transmission System with Different Wind Speed Regions during a Cyclone.

Table 4
Transmission Lines Located in Different Wind Regions.

Wind Speed Region	Transmission Lines Located in each of the Region	Total No. of Transmission Line (*RLi*)
High Wind Region	(8−9), (9−10), (9−11), (9−12), (9−13), (10−12), (11−13),(30−31),(31−32), (32−33),(34−32),(34−35),(35−36),(36−40), (11−41),(41−42),(41−43),(49−50),(50−51), (10−51),(54−55),(11−43),(40−56),(56−41), (56−42),(57−56),(9−55)	27
Medium Wind Region	(6−8),(13−14),(13−15),(7−8),(12−13), (12−16),(12−17), (19−20),(21−20), (21−22),(22−23),(23−24),(24−25), (24−25),(24−26),(28−29),(7−29),(25−30), (36−37),(37−38),(37−39),(22−38),(38−44), (46−47),(47−48),(48−49),(13−49),(29−52), (52−53),(53−54),(39−57),(38−49),(38−48)	33
Low Wind Region	(1−2), (2−3), (3−4), (4−5), (4−6),(6−7), (1−15),(1−16),(1−17), (3−15),(4−18), (4−18),(5−6),(14−15),(18−19), (26−27), (27−28),(15−45),(14−46),(44−45)	20

taken. As seen for base case, on day1 (D1), 10, 5, and 0 numbers of transmission lines have tripped and on day2 (D2) 13, 8 and 1 numbers of transmission lines have tripped in high, medium and low wind region respectively.

Fig. 8 illustrates the performance of transmission lines remaining in service (TL_{ser}) under varying robustness scenarios for Cyclone-1 over a 5-day period. The results show that higher robustness levels lead to significantly more transmission lines remaining operational, particularly in high wind regions where the impact of the cyclone is most severe. For instance, on Day 1, the TL_{ser} in the high wind region increases from 15 for the 20 % less robust scenario to 20 for the 20 % more robust scenario, reflecting the benefit of infrastructure hardening.

Similar trends are observed across medium and low wind regions, with the difference becoming more pronounced as the cyclone progresses. This comparative analysis underscores the critical role of robustness in ensuring the resilience of transmission networks during extreme weather events.

6.4.1. *Time-dependent resilience metrics during cyclone-1*

Table 6 presents the resilience metrics for transmission lines under different robustness levels (H_j) during the degradation state (State-II). The metrics include the hourly resilience degradation rate (R_{hour}) and the transmission line degradation level (TL_{dl}) across high (H), medium (M), and low (L) wind regions. The results indicate that higher robustness levels significantly reduce both the rate of resilience degradation and the number of transmission lines tripped. For instance, in the high wind region, R_{hour} improves from − 0.225 for H_1 (20 % less robust) to − 0.175 for H_5 (20 % more robust), while TL_{dl} decreases from 27 to 21. A similar trend is observed in medium and low wind regions, where the degradation rate and the number of tripped lines decline as robustness increases.

The resilience metric R_{dr} , evaluated using Eq. (17) during State-III, quantifies the duration for which transmission lines remain in a post-event degraded state. By varying the normal repair time (R_{base}) by ±10 % and ±20 %, responsiveness case scenarios (S_j) are proposed, with results presented in Table 7. for the 10 % more robust scenario. The data indicate that increasing responsiveness decreases the duration of the degraded state (R_{dr}) across all three wind regions. For instance, in

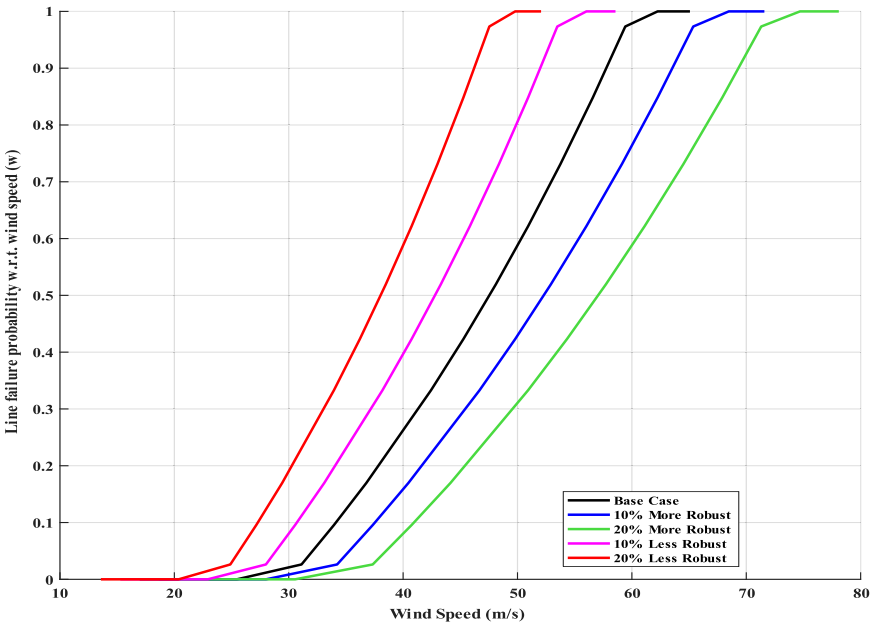

Fig. 5. Fragility Curves of Transmission Line in Base and Robust Cases.

Table 5
Maximum Wind Speed of cyclone-1 and cyclone-2.

Wind Region	Cyclone-1 (m/s)	Cyclone-2 (m/s)
High Wind Region	65	45
Medium Wind Region	54	41
Low Wind Region	42	33

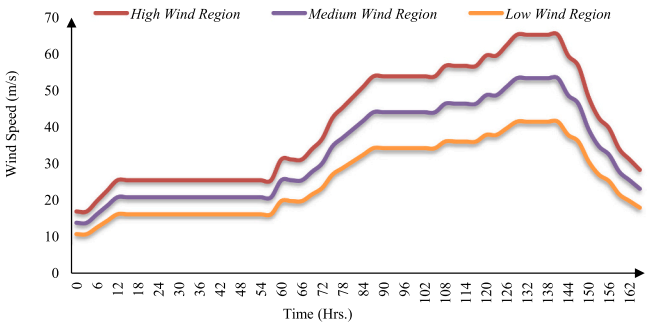

Fig. 6. Wind speed during cyclone-1 in high, medium and low wind region.

the high wind region, R_{dr} reduces from 33.72 h for S_1 (20 % less responsive) to 22.48 h for S_5 (20 % more responsive).

The metric R_{rs}, calculated using Eq. (18) during State-IV, measures the restoration rate, indicating how quickly transmission lines are repaired during the restoration phase. Table 7 shows that responsiveness adjustments have a notable impact on R_{rs}, with faster restoration rates observed for higher responsiveness levels. In the high wind region, R_{rs} increases from 0.4797 for S_1 to 0.7196 for S_5. However, the influence of robustness and responsiveness on restoration performance is limited, as R_{rs} largely depends on the availability of repair crews. Since the number of repair crews is assumed constant across all scenarios, the restoration times are primarily influenced by responsiveness adjustments rather than robustness enhancements.

6.4.2. Time-dependent resilience area metrics during cyclone-1

The Apart from above metrics, area metrics for cyclone-1 are also calculated with the help of multi state resilience curve. This is divided into three area, during state-II, state-III and state-IV and corresponding resilience area metrics are R_{Area_I} , $R_{Area_{II}}$ and $R_{Area_{III}}$ respectively. Larger area indicates that the impact of windstorm is more and vice versa. Result of resilience area metrics of different states are tabulated in Table 8 (for 10 % more robust case scenario). It is observed from the table that when transmission line is made more responsive by reducing the repair time, $R_{Area_{II}}$ and $R_{Area_{III}}$ decreases. The impact is more for higher wind speeds during the windstorm reflected through the area metrics. R_{Area_I} is constant as this do not depend on time to repair, R_{Time} as the event is in progress in State-II. These metrics capture the cumulative resilience during the degraded and restoration phases, reflecting the impact of increased robustness and responsiveness. The results provide insights into the effectiveness of hardening measures and repair strategies in minimizing system downtime and enhancing recovery.

6.5. Resilience of transmission lines during cyclone-2

Cyclone-2 data, obtained from the IMD, is described in detail in Section 2. Using the modeling framework outlined in Section 2, Cyclone-2 is depicted graphically in Fig. 9.

Fig. 10 presents the number of transmission lines tripped during Cyclone-2 under varying robustness scenarios across five days for high (H), medium (M), and low (L) wind regions. Similar to the results of Cyclone-1, higher robustness levels result in fewer tripped lines. However, since Cyclone-2 has a lower intensity than Cyclone-1, the overall number of tripped lines is reduced in all scenarios, reflecting the less severe impact of this event.

Fig. 11 illustrates the number of transmission lines in service during Cyclone-2 under five different robustness scenarios. It is evident that higher robustness levels (e.g., 20 % more robust) result in a greater number of transmission lines remaining in service, particularly in high wind regions, as these lines are better equipped to withstand the cyclone's impact. In contrast, lower robustness levels (e.g., 20 % less robust) show a significant drop in service levels, especially in high and medium wind regions. Compared to Cyclone-1, the overall impact is less severe for Cyclone-2, which is reflected in higher service levels across all scenarios due to its lower intensity.

6.5.1. Time-dependent resilience metrics during cyclone-2

Table 9. presents the time-dependent resilience metrics for

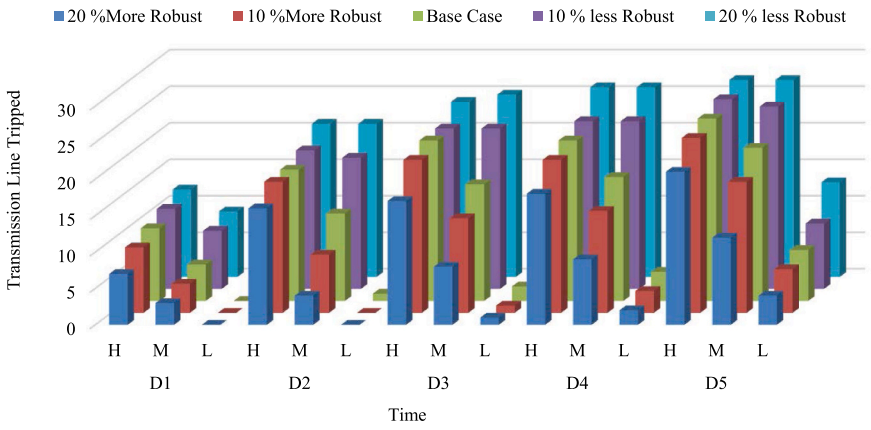

Fig. 7. Number of Transmission Line Tripped /Day.

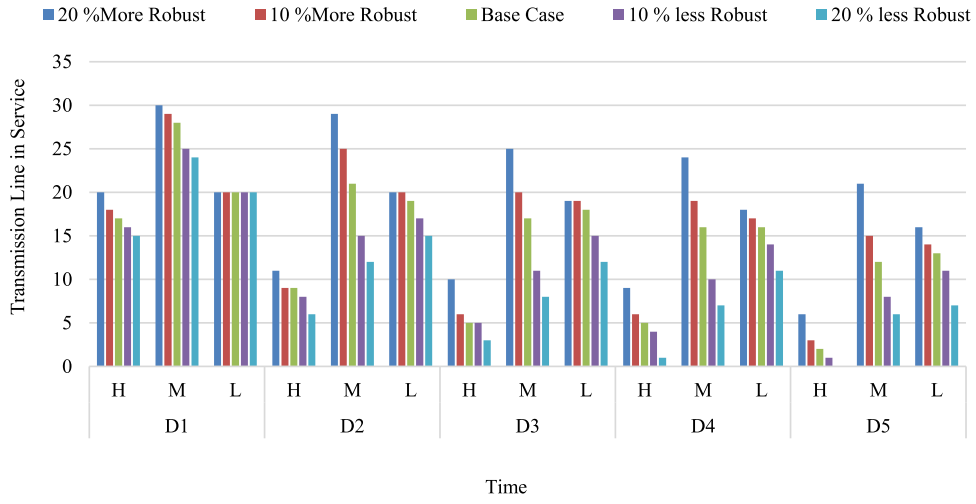

Fig. 8. Number of Transmission Line Remain in Service.

Table 6
Resilience Metrices for Transmission Line in Robust Case Scenario (State-II).

Robustness Level (H_j)	R_{hour}			TL_{dl}		
	H	M	L	H	M	L
H_1	−0.225	−0.225	−0.108	27	27	13
H_2	−0.216	−0.208	−0.075	26	25	9
H_3	−0.208	−0.175	−0.058	25	21	7
H_4	−0.200	−0.150	−0.050	24	18	6
H_5	−0.175	−0.100	−0.033	21	12	4

transmission lines during Cyclone-2 under robust case scenarios. Similarly, the results for Cyclone-1, this table highlights the degradation rate (R_{hour}) and the number of transmission lines down (TL_{dl}) across all wind regions for different robustness levels. However, due to the lower intensity of Cyclone-2, both the degradation rates and the number of lines down are notably smaller in comparison to Cyclone-1, indicating a less severe impact on the transmission network.

Table 10 summarizes the resilience metrics $R_{dr}$and R_{rs} for transmission lines during the response phase (State-III and State-IV) in the 10 % more robust scenario for Cyclone-2. Compared to Cyclone-1, the metrics reflect a faster recovery and reduced post-event degraded duration due to Cyclone-2's lower intensity. This demonstrates the effectiveness of increased robustness in mitigating the impact of less severe cyclones.

6.5.2. Resilience area metrics during cyclone-2

Table 11. presents the resilience area metrics for transmission lines in the response case scenario during the 10 % more robust case for cyclone 2. The table evaluates resilience in terms of the areas covered during different states of response: and the overall resilience area, R_{Area_I}, $R_{Area_{II}}$, $R_{Area_{III}}$ and Overall, area for high (H), medium (M), and low (L) wind regions. The results indicate that as the response level (S_j) improves (e.g., from 20 % less responsive (S_1) to 20 % more responsive (S_5), the overall resilience area ($R_{Area}^{Overall}$) increases for all wind regions. This is due to quicker recovery and reduced post-event degraded and restoration times. For instance, $R_{Area}^{Overall}$ for high wind regions decreases from 948.48 in S_1 to 792.32 in S_5, reflecting better resilience. This trend highlights how improved responsiveness directly enhances resilience across different wind conditions.

Table 7
Resilience Metrics for Transmission Lines in 10 % More Robust Scenario During Response Phase (State-III and State-IV).

Responsiveness Level (S_j)	R_{dr}			R_{rs}		
	H	M	L	H	M	L
S_1	33.72	35.33	27.28	0.4797	0.3765	0.1131
S_2	30.91	32.39	25.01	0.5233	0.4107	0.1233
S_3	28.10	29.44	22.74	0.5756	0.4518	0.1357
S_4	25.29	26.50	20.46	0.6396	0.5020	0.1507
S_5	22.48	23.55	18.19	0.7196	0.5648	0.1696

Table 8
Resilience Area Metrics for Transmission Lines in 10 % More Robust Scenario During Response Phase.

Responsiveness Level (S_j)	R_{Area_I}			$R_{Area_{II}}$			$R_{Area_{III}}$			$R_{Area}^{Overall}$		
	H	M	L	H	M	L	H	M	L	H	M	L
S_1	1440	1080	360	809.46	636.04	163.73	600.37	430.26	159.21	2849.83	2146.30	682.94
S_2	1440	1080	360	742.00	583.03	150.08	550.34	394.41	145.94	2732.35	2057.44	656.03
S_3	1440	1080	360	674.55	530.03	136.44	500.31	358.55	132.68	2614.86	1968.59	629.12
S_4	1440	1080	360	607.09	477.03	122.79	450.28	322.69	119.41	2497.37	1879.73	602.21
S_5	1440	1080	360	539.64	424.02	109.15	400.24	286.84	106.14	2379.89	1790.87	575.29

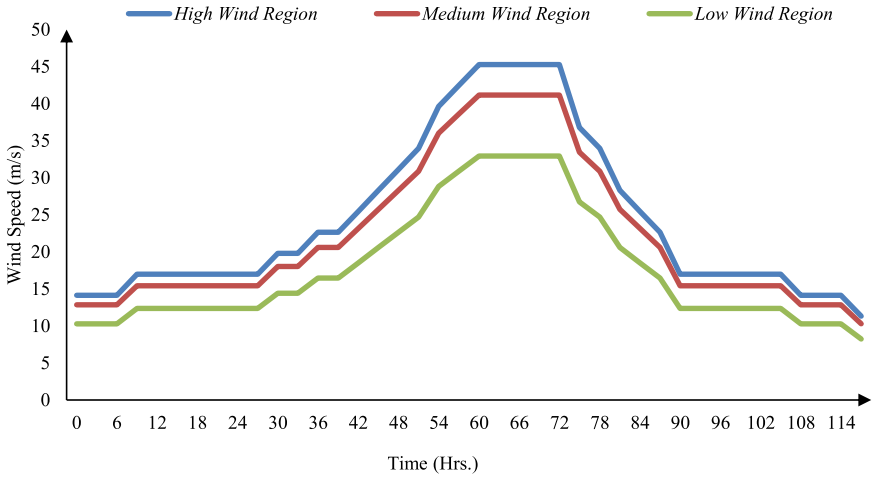

Fig. 9. Wind speed during cyclone-2 in high, medium and low wind region.

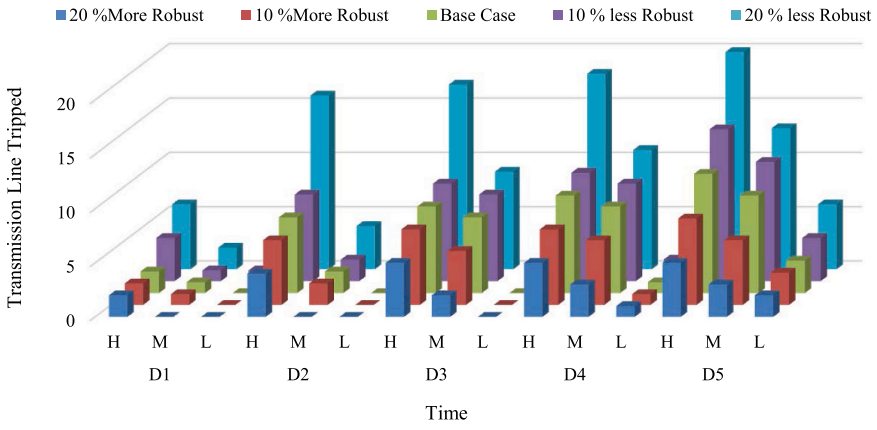

Fig. 10. Number of Transmission Line Tripped /Day.

6.6. Results for proposed cost analysis

This cost analysis study has been conducted only for the case study during Cyclone-1. The results for the base case and robustness case are considered only in the context of Cyclone-1, as previously discussed in section 6.4.

6.6.1. Analysis of robustness cost

Taable-12 presents the cost estimates for constructing or upgrading transmission lines designed to withstand increasing wind speeds. The values are extracted from utility planning cost references and represent the cost per unit length required to achieve various design wind speed thresholds, which are directly related to the structural robustness of transmission infrastructure (The Cost of Climate Change on Transmission Infrastructure', ASCE, 2022).

Fig. 12 illustrates how the total transmission line cost per kilometre increases with higher design wind speed thresholds, highlighting that the incremental cost of robustness upgrades becomes more significant as wind resistance requirements grow beyond the base case (140 mph or 62.6 m/s).

Table 13 shows cost per unit increase in design wind speed (α) required to increase the design wind speed of transmission lines within specific wind speed ranges. The values reflect that reinforcement costs vary non-linearly, with the highest unit cost observed in the lower wind speed range (62.6–67.06 m/s).

Table 14 presents the robustness cost per kilometre required to harden transmission lines in different wind regions. It shows that as robustness increases (by 3.4 m/s and 9.4 m/s), the cost of structural upgrades rises significantly, with high wind regions demanding the greatest investment due to their exposure to more severe wind conditions.

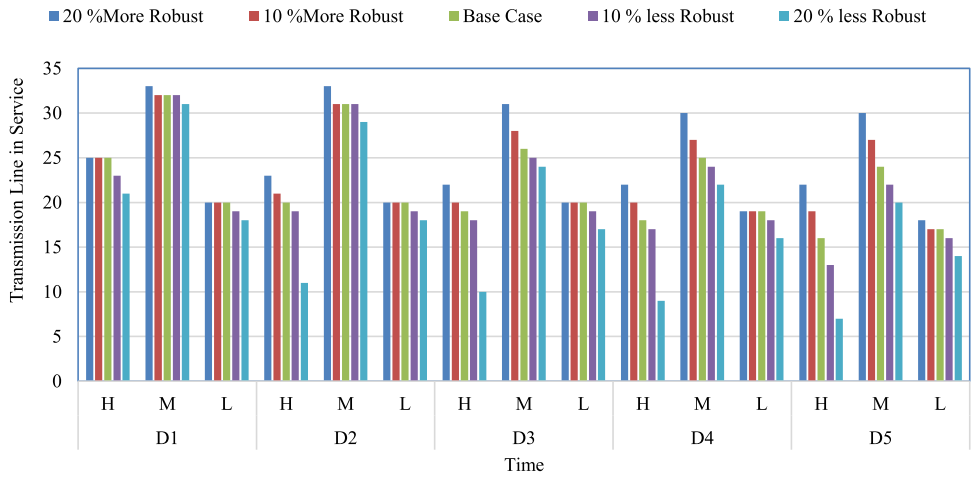

Fig. 11. Number of Transmission Line Remain in Service.

Table 9
Resilience Metrices for Transmission Line in Robust Case Scenario (State-II).

Robustness Level (H_j)	R_{hour}			TL_{dl}		
	H	M	L	H	M	L
H_1	−0.166	−0.108	−0.050	20	13	6
H_2	−0.166	−0.091	−0.033	14	11	4
H_3	−0.091	−0.075	−0.025	11	9	3
H_4	−0.067	−0.050	−0.025	8	6	3
H_5	−0.041	−0.025	−0.017	5	3	2

Table 10
Resilience Metrics for Transmission Lines in 10 % More Robust Scenario During Response Phase (State-III and State-IV).

Responsiveness Level (S_j)	R_{dr}			R_{rs}		
	H	M	L	H	M	L
S_1	37.67	39.13	62.88	0.1916	0.1489	0.1574
S_2	34.53	35.87	57.64	0.2090	0.1624	0.1717
S_3	31.39	32.61	52.40	0.2299	0.1786	0.1888
S_4	28.25	29.35	47.16	0.2554	0.1985	0.2098
S_5	25.11	26.09	41.92	0.2873	0.2233	0.2360

6.6.2. Analysis of responsiveness cost

From Table 7 it can be observed that improving responsiveness reduces the average outage duration across all wind regions. A 20 % improvement in repair efficiency leads to faster recovery. Table 15 quantifies the responsiveness cost per kilometre for reducing repair time in different wind regions under 10 % and 20 % improvement scenarios. As expected, higher responsiveness (greater Δr) leads to increased cost, with high wind regions contributing the most due to a larger number of affected lines and longer baseline repair times.

6.6.3. Failure cost analysis

Table 16 shows that enhancing robustness significantly reduces failure impacts: both Load Not Served (LNS) and Energy Not Served (ENS) decrease with higher robustness levels. Consequently, the total failure cost drops by over 35 % with 10 % robustness and nearly 68 % with 20 % robustness, highlighting the economic benefit of structural hardening.

6.7. Results for economic evaluation metrics

6.7.1. Benefit metric results

Table 17 presents the total economic performance of different resilience strategies by combining robustness cost, responsiveness cost and failure cost to compute the total cost.

Although failure costs reduce substantially with higher robustness, the overall total cost increases significantly due to the high capital investment in hardening and responsiveness. As a result, both 10 % and 20 % robustness scenarios yield negative net benefits, indicating that the cost of resilience upgrades exceeds the monetary value of avoided outages in these scenarios when measured purely in USD/km terms. This highlights the importance of cost-effectiveness analysis in resilience planning.

In above table Even though failure cost per km drops sharply (from $14.6k to $4.7k), the added cost per km for robustness and responsiveness is extremely high. This leads to a negative net benefit per km, unless the robustness is applied only to critical segments, not the full system.

6.7.2. Results for cost-benefit trade-off curve

This section analyses the trade-off between the total cost of implementing resilience strategies and the resilience gain, defined as the amount of energy not served (ENS) avoided due to hardening and faster recovery measures.

In Fig. 13 shows, the cost per km grows exponentially with robustness Even small increases in robustness (10 %) lead to large jumps in cost. This curve visually supports the conclusion that selective or strategic hardening is more practical than system-wide upgrades. As shown in the Fig. 13, the cost-benefit trade-off curve plots total cost per

Table 11
Resilience Area Metrics for Transmission Lines in 10 % More Robust Scenario During Response Phase.

Responsiveness Level (S_j)	R_{Area_I}			$R_{Area_{II}}$			$R_{Area_{III}}$			$R_{Area}^{Overall}$		
	H	M	L	H	M	L	H	M	L	H	M	L
S_1	480	360	180	301.43	234.83	188.66	167.04	120.91	28.59	948.48	715.74	397.26
S_2	480	360	180	276.31	215.26	172.94	153.12	110.83	26.21	909.44	686.09	379.15
S_3	480	360	180	251.19	195.69	157.22	139.20	100.75	23.83	870.40	656.45	361.05
S_4	480	360	180	226.07	176.12	141.49	125.28	90.68	21.44	831.36	626.80	342.94
S_5	480	360	180	200.95	156.55	125.77	111.36	80.60	19.06	792.32	597.16	324.84

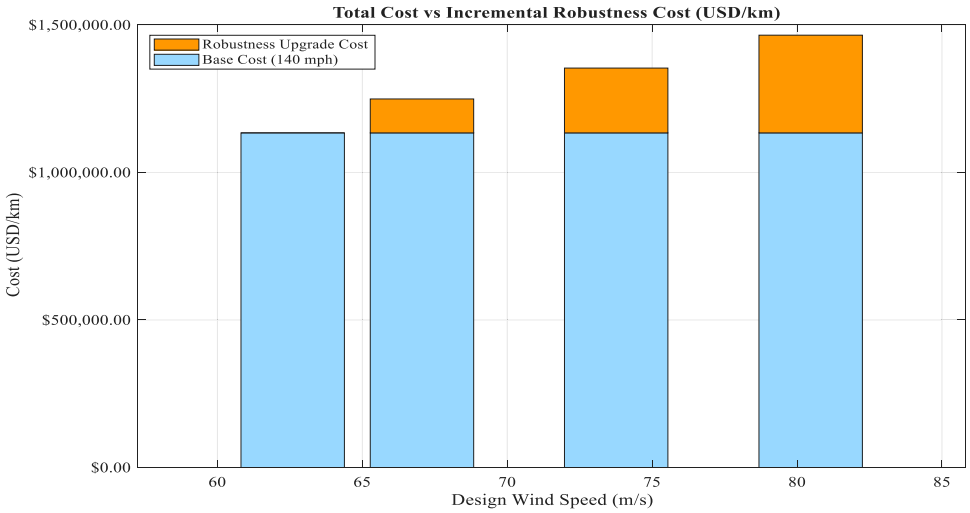

Fig. 12. Total Cost vs. Robustness Cost.

Table 12
Transmission Line Cost at Different Design Wind Speed.

Design Wind Speed (mph)	Design Wind Speed (m/s)	Cost ($/mile)	Cost ($/km)
140	62.60	$1824,600	$1134,195
150	67.06	$2011,000	$1249,191
165	73.76	$2179,000	$1353,871
180	80.47	$2358,500	$1465,368

kilometre (USD/km) against resilience gain (MWh Energy Saved) for three scenarios: Base, 10 % Robust, and 20 % Robust. The base case has no investment in resilience and consequently zero resilience gain, serving as a reference point.

The curve is steep and nonlinear, showing rapidly increasing cost for each unit of resilience gain. The Base point (0 gain, lowest cost) is the reference. 10 % Robustness provides moderate resilience gain (4416 MWh) at significant cost. 20 % Robustness offers more gain (7939.2 MWh). This trend highlights that while resilience gains increase with robustness, the marginal cost of avoided ENS rises, making it crucial to balance resilience performance with economic efficiency.

6.7.3. Results for economic metrics

Table 18 presents three key economic indicators-Cost Effectiveness Ratio (CER), Benefit-to-Cost Ratio (BCR), and Resilience Efficiency Index (REI)-to evaluate the economic performance of 10 % and 20 % robustness scenarios:

(i) CER (USD/km/MWh) represents the cost incurred per unit of resilience gained. A lower CER indicates a more efficient strategy. The 20 % robustness case shows slightly lower CER ($968.91/km/MWh) compared to 10 %, implying better cost efficiency.
(ii) BCR compares the monetary benefit (avoided failure cost) to the investment in robustness and responsiveness. Both scenarios show BCR values much lower than 1 (0.0012 and 0.0013), indicating that the costs outweigh direct financial benefits under the given assumptions.

Table 13
Values of α within specific wind speed ranges (USD/km/(m/s)).

Wind Speed Range (m/s)	α (USD/km/(m/s))
62.6–67.06	26,012.87
67.06–73.76	15,635.00
73.76–80.47	16,704.62

Table 14
Robustness Cost (USD/km).

Region	Base (0 m/s)	10 % Robustness (3.4 m/s)	20 % Robustness (9.4 m/s)
High Wind Region	$0	$2.12 M/km	$4.06 M/km
Medium Wind Region	$0	$1.59 M/km	$2.32 M/km
Low Wind Region	$0	$0.53 M/km	$0.77 M/km

(iii) REI (MWh per $1 M/km) quantifies how many MWh of energy disruption are avoided per million dollars invested per km. The 20 % robust case yields a higher REI (1032.56 MWh), signifying it is slightly more resilience-efficient than the 10 % case.

Although the 20 % robust scenario provides a marginally better economic return per unit of resilience, both strategies yield low BCR, suggesting that such investments are more justified when viewed from a resilience assurance perspective rather than immediate economic return.

Table 15
Responsiveness Cost for Each Wind Region Scenario (USD/km).

Region	Lines Affected	10 % Responsiveness		20 % Responsiveness	
		Δr (hrs)	C_{resp} (USD/km)	Δr (hrs)	C_{resp} (USD/km)
High Wind Region	24	2.81	$134,880	5.62	$269,760
Medium Wind Region	18	2.94	$105,840	5.89	$212,040
Low Wind Region	6	2.28	$27,360	4.55	$54,600
Total C_{resp} (USD/km)			$268,080		$536,400

Table 16
Failure Cost (USD/km).

Metric	Base Case	10 % Robust	20 % Robust
Total LNS (MW)	488	304	157.2
Total ENS (MWh)	11,712	7296	3772.8
Total C_{fail} (USD/km)	$117.12 M	$72.96 M	$37.73 M

Table 17
Total Economic Performance (USD/km).

Scenario	C_{rob}	C_{resp}	C_{fail}	C_{Tot}	B_{net}
Base	$0	$0	$14,640	$14,640	—
10 % Robust	$4240,000	$268,080	$9120	$4517,200	$4502,560
20 % Robust	$7150,000	$536,400	$4716	$7691,116	$7676,476

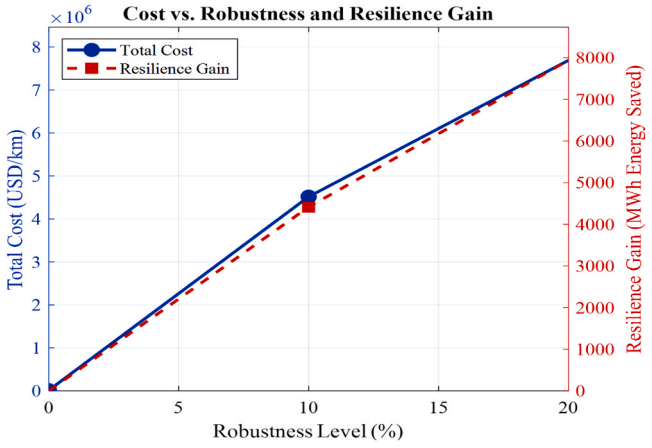

Fig. 13. Cost-Benefit Trade-Off Curve.

6.8. Results for sensitivity analysis

This section evaluates how variations in key economic and design parameters influence the total cost and economic viability of transmission line resilience strategies. The goal of the sensitivity analysis is to identify the parameters that most significantly affect resilience outcomes and investment decisions.

6.8.1. Purpose of sensitivity analysis

Power system planners operate under uncertainty regarding material costs, value of lost load (VOLL), and achievable robustness. Sensitivity analysis helps:

- Assess the stability and robustness of the cost-benefit conclusions.
- Identify critical cost drivers (e.g., α, VOLL).
- Provide a range of economic outcomes under different realistic assumptions.

6.8.2. Parameters considered

The following three parameters were varied across a range of reasonable values:

Based on the variable shown in Table 19, sensitivity formula can be derived from Eq. (39).

$$S_{f,\ x} = \frac{f_2 - f_1}{x_2 - x_1} \times \frac{x_1}{f_1} = \frac{\Delta f}{\Delta x} \times \frac{x_1}{f_1} \tag{39}$$

Where f_1 , f_2 are output value before and after a change and x_1 , x_2 are input parameter values before and after change. Here consider input and output parameters are:

f : output parameter (C_{Tot} , B_{net}, REI, CER) and x : input parameter (α, VOLL, Δv_{des}, No. of Lines)

Table 18
CER, BCR and REI.

Metric	10 % Robust	20 % Robust
CER (USD/km/MWh)	$1022.89	$968.91
BCR	0.0012	0.0013
REI (MWh per $1 M/km)	978.02	1032.56

Table 19
Sensitivity Parameters.

Parameter	Description	Variation
α (USD/km/m/s)	Cost per unit increase in design wind speed. (material cost uncertainty)	±10 % of base value (23,412−28,614)
VOLL(USD/MWh)	Value of lost load (economic loss per MWh not served)	5000 / 10,000 / 20,000
Δv_{des}(m/s)	Increase in design wind speed (in m/s) due to line hardening.	3.4 m/s (10 % robust), 9.4 m/s (20 % robust)
No. of Lines	Base case, 10 % robust case and 20 % robust case	53 (Base) → 48 (10 %) → 37 (20 %)

6.8.3. Sensitivity analysis results

Table. 20 presents the outcomes of a detailed sensitivity analysis evaluating how variations in key economic parameters: namely the cost per unit increases in design wind speed (α), the value of lost load (VOLL), and the Increase in design wind speed (in m/s) due to line hardening Δv_{des}: affect the overall economic performance of transmission system resilience strategies. The base case (no hardening or responsiveness), only failure cost contributes to the total cost, and no resilience gain is achieved.

In contrast, the 10 % robustness scenario (Δv_{des} = 3.4 m/s) with different α values shows that as α increases from $23,412 to $28,614 USD/km/m/s, the robustness cost rises significantly, leading to a steady increase in total cost and a corresponding decline in net benefit and resilience efficiency (REI). The cost-effectiveness ratio (CER) worsens from 12.89 to 15.29 USD/km/MWh, indicating reduced economic efficiency. Similarly, the 20 % robustness scenario (Δv_{des} = 9.4 m/s) shows a larger robustness cost due to more aggressive hardening. While this results in lower failure costs and improved resilience performance, the economic trade-off becomes less favorable as α increases, with CER values rising from 13.42 to 16.27 and REI declining from 74,501 to 61,457 MWh per $1 million/km. These results suggest that although higher robustness levels provide better protection, they do so at an increasing cost and may yield diminishing economic returns. Overall, the sensitivity analysis highlights that the system's economic and resilience performance is most sensitive to changes in α and confirms that moderate hardening strategies (e.g., 10 % robust) may offer the best balance between cost and resilience under uncertain conditions. Decision-makers must balance robustness level with α and VOLL to optimize cost-efficiency in resilience planning.

Table 21 summarizes the sensitivity of key parameters affecting economic resilience outcomes. It highlights that VOLL and α (cost per unit increase in design wind speed) have the highest impact, while Δv_{des}(design wind speed increment) and number of lines hardened show moderate to low sensitivity, guiding more cost-effective resilience planning. The results of the sensitivity analysis are summarized in Table 21 with corresponding strategic actions, while Fig. 14 (radar chart) provides a visual comparison of each parameter's influence on net benefit. Both confirm that VOLL and α are the most critical economic drivers, while Δv_{des} and the number of lines hardened have more limited sensitivity.

7. Conclusions

In this paper, the quantitative assessment of infrastructure resilience of transmission lines has been evaluated using multiple resilience metrics when subjected to extreme weather events such as severe cyclones of varying intensities. Ensuring the robustness and rapid response of transmission lines against cyclonic disruptions is shown to be crucial for maintaining overall grid performance and service continuity. A multi-state resilience curve was employed to characterize the degradation and recovery trajectory of the system, and resilience metrics were derived for each state to quantify performance. A novel bi-level resilience framework is proposed for IEEE 57-bus system. The first level of

Table 20
Sensitivity Analysis Results.

Scenario	α (USD/km/m/s)	VOLL (USD/MWh)	Δv_{des} (m/s)	Lines Hardened	C_{rob} (USD/km)	C_{resp} (USD/km)	C_{fail} (USD/km)	C_{Tot} (USD/km)	B_{net} (USD/km)	REI (MWh/$1 m/km)	CER (USD/km/MWh)
Base	23412	5000	0.0	53	0	0	7320	7320	0	0.00	—
Base	23412	10000	0.0	53	0	0	14,640	14,640	0	0.00	—
Base	23412	20000	0.0	53	0	0	29,280	29,280	0	0.00	—
10 %	23412	10000	3.4	48	47,760	33.51	9120	56,913	42,273	77,592	12.89
10 %	26013	10000	3.4	48	53,066	33.51	9120	62,220	47,580	70,974	14.09
10 %	28614	10000	3.4	48	58,373	33.51	9120	67,526	52,886	65,397	15.29
20 %	23412	10000	9.4	37	101,780	67.05	4716	106,563	91,925	74,501	13.42
20 %	26013	10000	9.4	37	113,090	67.05	4716	117,873	103,230	67,353	14.85
20 %	28614	10000	9.4	37	124,400	67.05	4716	129,191	114,540	61,457	16.27

Table 21
Prioritized Sensitivity Summary.

Rank	Parameter	Sensitivity	Strategic Action
1	VOLL	Very High	Prioritize resilience in high-VOLL areas (e.g., urban/load centers) as avoided outage value has the greatest effect on net benefit.
2	α	High	Minimize hardening costs by using cost-efficient materials and targeting only high-risk regions.
3	Lines Hardened	Moderate	Use criticality-based line selection to optimize the trade-off between coverage and cost.
4	Δv_{des}	Low–Moderate	Avoid excessive hardening beyond 10–15 %, as marginal resilience gain does not justify the rising cost.

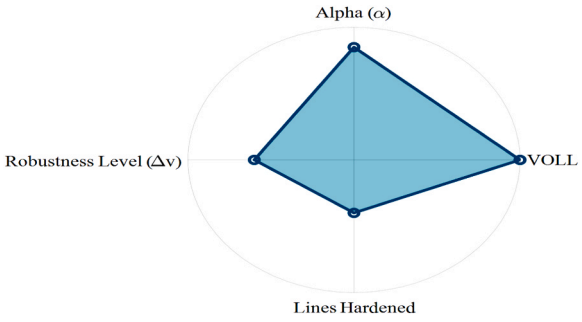

Fig. 14. Sensitivity Impact on Net Benefit.

the framework addresses robustness (infrastructure hardening), and the second level focuses on responsiveness (repair efficiency). Simulation results clearly demonstrate the framework's capability to evaluate the resilience of transmission networks under multiple cyclone scenarios. The analysis revealed that transmission lines in higher wind speed regions experienced greater failures, emphasizing the need for targeted resilience enhancement measures. To further enrich the framework, this study incorporated a detailed cost modelling approach comprising:

- Robustness cost calculated using piecewise linear α-values derived from transmission line hardening cost data.
- Responsiveness cost, based on reductions in repair time and estimated β-values.
- Failure cost, quantified from actual simulation results using Load Not Served (LNS), energy not served (ENS), and assumed VOLL values.

Additionally, multiple economic performance metrics and Resilience Efficiency Index (REI) were calculated for each scenario. These enabled the comparison of different resilience strategies from a techno-economic perspective. A comprehensive sensitivity analysis was also performed to assess how variations in key economic driver's impact investment decisions. The findings confirm that moderate hardening (10 % robustness) often provides the best cost-benefit trade-off under typical economic assumptions. The proposed framework and modeling approach are therefore highly relevant for power system planners, offering a practical decision-making tool to assess, compare, and economically justify resilience investments in transmission infrastructure. Future work may focus on integrating optimization models to automatically identify cost-optimal resilience strategies and expanding the framework to include distribution networks and real-time adaptive resilience planning under uncertainty.

Key finding

- **Effectiveness of Hardening:** Increasing the design wind speed (v_{des}) through hardening substantially reduces failure costs and enhances resilience. failure cost per km drops sharply (from $14.6k to $4.7k) at 20 % hardening.
- **Economic Viability:** Despite higher hardening costs (α), both the net benefit (B_{net}) and cost-effectiveness ratio (CER) remain favorable, confirming that resilience investment is economically justified.
- **Dominant Role of Robustness:** Both robustness and responsiveness contribute to resilience improvement, but robustness emerges as the primary driver under severe storm intensities, reinforcing the importance of structural strengthening.
- **Improved Resilience Indices:** The resilience enhancement index (REI) increases from 978.02 MWh/$1 m/km (10 % hardening) to 1032.56 MWh/$1m/km (20 % hardening), highlighting the incremental effectiveness of resilience strategies in safeguarding transmission systems against cyclones.

Practical implications

The proposed bi-level multi-state resilience framework offers several practical implications for the planning and operation of power transmission systems under extreme weather events:

- **Support for Investment and Policy Decisions:** The methodology provides quantitative metrics, robustness, responsiveness, and cost-integrated resilience that help utilities and policymakers identify the most cost-effective resilience strategies. By comparing outage costs with infrastructure hardening investments, decision-makers can optimize resource allocation and prioritize reinforcement of critical transmission lines.
- **Enhanced Risk Assessment and Emergency Preparedness:** By using fragility curves, failure probabilities, and Monte Carlo Simulation, the framework enables operators to predict potential transmission line failures under varying cyclone intensities. This knowledge strengthens disaster preparedness by allowing utilities to anticipate vulnerabilities, allocate repair crews efficiently, and minimize restoration times.

- **Economic Evaluation of Resilience Measures:** The integration of economic drivers such as unit hardening costs (α), Value of Lost Load (VOLL), and changes in design wind speed (Δv_{des}) allows for a balanced trade-off between reliability and cost-effectiveness. This ensures that resilience planning is financially viable, making it attractive for utility companies and regulatory bodies.
- **Real-World Relevance and Demonstration:** Application of the framework on the IEEE 57-bus test system validates its feasibility and demonstrates its transferability to real-world transmission networks. This makes the framework an actionable tool for power system operators facing increasing threats from cyclones and other High-Impact Low-Probability (HILP) events.

Future work

While the present study demonstrates the applicability of the proposed bi-level resilience framework using simulated failures informed by fragility curves and cyclone wind data from the IMD, validation against real-world outage records remains an important next step. Due to the limited availability of high-resolution tripping and restoration data from utilities (often restricted for confidentiality reasons), this work has based on probabilistic estimation to model line failures and recovery patterns.

In future research, the methodology will be extended and benchmarked against actual outage records from historical cyclonic events. This comparison of predicted vs. observed line tripping rates and recovery durations will provide empirical validation, ensuring the robustness and practical adoption of the framework by utilities.

CRediT authorship contribution statement

Kusum Verma: Writing – review & editing, Supervision, Investigation, Validation, Visualization. **Abhishek Kumar Gupta:** Writing – original draft, Validation, Methodology, Conceptualization. **Sachin Sharma:** Writing – review & editing, Validation, Investigation, Supervision.

Declaration of Competing Interest

The authors declare that they have no known competing financial interests or personal relationships that could have appeared to influence the work reported in this paper.

Data availability

No data was used for the research described in the article.

References

A Report on Extremely Severe Cyclonic Storm FANI over the Bay of Bengal (26 April to 4 May 2019), 'Government of India Ministry Of Earth Sciences India Meteorological Department ', May 2019.

Amrovani, M.A., Askarian-Abyaneh, H., Gharibi, M.A., Mozaffari, M., 2025. Urban grid resilience assessment framework: leveraging electric vehicles, time-based analysis, and mobile distributed generators for repair crew strategic deployment (Mar). Sustain. Energy Grids Netw. 41, 101588. https://doi.org/10.1016/j.segan.2024.101588.

Baburaj, P.P., Abhilash, S., Abhiram Nirmal, C.S., Sreenath, A.V., Mohankumar, K., Sahai, A.K., 2022. Increasing incidence of Arabian Sea cyclones during the monsoon onset phase: its impact on the robustness and advancement of Indian summer monsoon (Apr). Atmos. Res 267, 105915. https://doi.org/10.1016/j.atmosres.2021.105915.

Bhusal, N., Abdelmalak, M., Kamruzzaman, M., Benidris, M., 2020. Power system resilience: current practices, challenges, and future directions. IEEE Access 8, 18064–18086. https://doi.org/10.1109/ACCESS.2020.2968586.

Billinton, R., Li, W., 1994. Reliability assessment of electric power systems using Monte Carlo methods. Springer US, Boston, MA. https://doi.org/10.1007/978-1-4899-1346-3.

Bolan, S., et al., 2024. Impacts of climate change on the fate of contaminants through extreme weather events (Jan). Sci. Total Environ. 909, 168388. https://doi.org/10.1016/j.scitotenv.2023.168388.

Dunn, S., Wilkinson, S., Alderson, D., Fowler, H., Galasso, C., 2018. Fragility curves for assessing the resilience of electricity networks constructed from an extensive fault database (Feb). Nat. Hazards Rev. 19 (1), 04017019. https://doi.org/10.1061/(ASCE)NH.1527-6996.0000267.

Gama Dessavre, D., Ramirez-Marquez, J.E., Barker, K., 2016. Multidimensional approach to complex system resilience analysis (May). Reliab. Eng. Syst. Saf. 149, 34–43. https://doi.org/10.1016/j.ress.2015.12.009.

Guidotti, R., Chmielewski, H., Unnikrishnan, V., Gardoni, P., McAllister, T., Van De Lindt, J., 2016. Modeling the resilience of critical infrastructure: the role of network dependencies (Nov). Sustain. Resilient Infrastruct. 1 (3–4), 153–168. https://doi.org/10.1080/23789689.2016.1254999.

Gupta, A.K., Verma, K., 2022. A probabilistic approach to assess quantitative resilience of transmission line during cyclone. In: IEEE 10th Power India International Conference (PIICON), . 2022. IEEE, New Delhi, India, pp. 1–6. https://doi.org/10.1109/PIICON56320.2022.10045228.

Gupta, A.K., Verma, K., 2024. MCS-ML based line vulnerability for infrastructural resilience assessment with multi-wind speed cyclonic zones (Nov). Comput. Electr. Eng. 119, 109575. https://doi.org/10.1016/j.compeleceng.2024.109575.

Lee, S.M., Chinthavali, S., Bhusal, N., Stenvig, N., Tabassum, A., Kuruganti, T., 2024. Quantifying the power system resilience of the US power grid through weather and power outage data mapping. IEEE Access 12, 5237–5255. https://doi.org/10.1109/ACCESS.2023.3347129.

Lian, X., Qian, T., Li, Z., Chen, X., Tang, W., 2023. Resilience assessment for power system based on cascading failure graph under disturbances caused by extreme weather events (Feb). Int. J. Electr. Power Energy Syst. 145, 108616. https://doi.org/10.1016/j.ijepes.2022.108616.

Liu, X., Xie, Q., 2024. A multi-model probabilistic framework to evaluate seismic resilience of UHV converter stations (Feb). Eng. Struct. 300, 117153. https://doi.org/10.1016/j.engstruct.2023.117153.

Liu, X., Wu, S., Xie, Q., Li, Q., 2024. Vulnerability-based seismic resilience and post-earthquake recovery assessment for substation systems (Nov). Structures 69, 107387. https://doi.org/10.1016/j.istruc.2024.107387.

Mohanty, S.K., Chatterjee, R., Shaw, R., 2020. Building resilience of critical infrastructure: a case of impacts of cyclones on the power sector in odisha (Jun). Climate 8 (6), 73. https://doi.org/10.3390/cli8060073.

Mujjuni, F., Betts, T.R., Blanchard, R.E., 2023. Evaluation of power systems resilience to extreme weather events: a review of methods and assumptions. IEEE Access 11, 87279–87296. https://doi.org/10.1109/ACCESS.2023.3304643.

Ouyang, M., Dueñas-Osorio, L., May 2014. Multi-dimensional hurricane resilience assessment of electric power systems. Struct. Saf. 48, 15–24. https://doi.org/10.1016/j.strusafe.2014.01.001.

Panteli, M., Pickering, C., Wilkinson, S., Dawson, R., Mancarella, P., 2017. Power system resilience to extreme weather: fragility modeling, probabilistic impact assessment, and adaptation measures (Sep). IEEE Trans. Power Syst. 32 (5), 3747–3757. https://doi.org/10.1109/TPWRS.2016.2641463.

Regional Specialized Meteorological Centre for Tropical Cyclones Over North Indian Ocean, 'RSMC'. Accessed: Oct. 13, 2023. [Online]. Available: ⟨https://rsmcnewdelhi.imd.gov.in/⟩.

Resilience-oriented Transmission Expansion Planning with Optimal Transmission Switching Under Typhoon Weather', *CSEE J. Power Energy Syst.*, 2024, doi: 10.17775/CSEEJPES.2021.07840.

Sharma, N., Tabandeh, A., Gardoni, P., 2018. Resilience analysis: a mathematical formulation to model resilience of engineering systems (Apr). Sustain. Resilient Infrastruct. 3 (2), 49–67. https://doi.org/10.1080/23789689.2017.1345257.

Singh, V., et al., 2021. Predicting the rapid intensification and dynamics of pre-monsoon extremely severe cyclonic storm "Fani" (2019) over the Bay of Bengal in a 12-km global model (Jan). Atmos. Res 247, 105222. https://doi.org/10.1016/j.atmosres.2020.105222.

Stanković, A.M., et al., 2023. Methods for analysis and quantification of power system resilience (Sep). IEEE Trans. Power Syst. 38 (5), 4774–4787. https://doi.org/10.1109/TPWRS.2022.3212688.

The Cost of Climate Change on Transmission Infrastructure', ASCE (2022). [Online]. Available: ⟨https://asec-engineers.com/the-cost-of-climate-change-on-transmission-infrastructure/⟩.

Tian, L., Yang, M., Liu, S., Liu, J., Gao, G., Yang, Z., 2023. Collapse failure analysis and fragility analysis of a transmission tower-line system subjected to the multidimensional ground motion of different input directions (Feb). Structures 48, 1018–1028. https://doi.org/10.1016/j.istruc.2023.01.042.

Trakas, D.N., Hatziargyriou, N.D., Panteli, M., Mancarella, P., 2016. A severity risk index for high impact low probability events in transmission systems due to extreme weather. In: IEEE PES Innovative Smart Grid Technologies Conference Europe (ISGT-Europe), 2016. IEEE, Ljubljana, Slovenia, pp. 1–6. https://doi.org/10.1109/ISGTEurope.2016.7856188 (Oct).

Umunnakwe, A., Huang, H., Oikonomou, K., Davis, K.R., 2021. Quantitative analysis of power systems resilience: standardization, categorizations, and challenges (Oct). Renew. Sustain. Energy Rev. 149, 111252. https://doi.org/10.1016/j.rser.2021.111252.

Wang, C., Ju, P., Wu, F., Pan, X., Wang, Z., 2022a. A systematic review on power system resilience from the perspective of generation, network, and load (Oct). Renew. Sustain. Energy Rev. 167, 112567. https://doi.org/10.1016/j.rser.2022.112567.

Wang, H., Hou, K., Zhao, J., Yu, X., Jia, H., Mu, Y., 2022b. Planning-Oriented resilience assessment and enhancement of integrated electricity-gas system considering multi-type natural disasters (Jun). Appl. Energy 315, 118824. https://doi.org/10.1016/j.apenergy.2022.118824.

Yang, R., Li, Y., 2022. Resilience assessment and improvement for electric power transmission systems against typhoon disasters: a data-model hybrid driven approach (Nov). Energy Rep. 8, 10923–10936. https://doi.org/10.1016/j.egyr.2022.08.226.

Yodo, N., Arfin, T., 2021. A resilience assessment of an interdependent multi-energy system with microgrids (Mar). Sustain. Resilient Infrastruct. 6 (1–2), 42–55. https://doi.org/10.1080/23789689.2019.1710074.

Zeng, X., et al., 2024. Highly-efficient single-level robust transmission expansion planning approach applicable to large-scale renewable energy integration (Sep). Sustain. Energy Grids Netw. 39, 101486. https://doi.org/10.1016/j.segan.2024.101486.

Zhuang, Y., Xie, Q., 2024. MILP-based framework for seismic resilience evaluation and enhancement of substations (Oct). Eng. Struct. 316, 118497. https://doi.org/10.1016/j.engstruct.2024.118497.